



Recent nationwide climate change impact assessments of natural hazards in Japan and East Asia

Nobuhito Mori^a, Tetsuya Takemi^a, Yasuto Tachikawa^b, Hirokazu Tatano^a, Tomoya Shimura^a, Tomohiro Tanaka^b, Toshimi Fujimi^c, Yukari Osakada^a, Adrean Webb^{a,*}, Eiichi Nakakita^a

^a Disaster Prevention Research Institute, Kyoto University, Kyoto, Japan

^b Graduate School of Engineering, Kyoto University, Kyoto, Japan

^c Graduate School of Engineering, Kumamoto University, Kumamoto, Japan

ARTICLE INFO

Keywords:

Global warming
Natural disasters
Impact assessment
Downscaling
Extreme events
Heavy precipitation
River flooding
Coastal hazards
Economic loss

ABSTRACT

Climate change due to global warming is expected to have major impacts on phenomena such as tropical cyclones (TCs), Baiu, precipitation, and seasonal storms. Many natural disasters in East Asia are driven by TC (typhoon) activity in particular and their associated hazards are sensitive to local-scale characteristics. As such, it is critically important to numerically simulate TC activity (and other phenomenon) on local scales in order to properly assess climate change impacts on natural hazards in the region. In addition, projecting future changes of many TC-related hazards and/or their potential economic impacts can be challenging due to their low occurrence frequencies in any one particular area. With these views in mind, a collaborative research program was formed in Japan to project long-term changes in natural hazards in Japan and East Asia based on local-scale and large-ensemble numerical experiments. This paper reviews recent climate change impact assessments (written in both English and Japanese) from the program and summarizes the projected future changes in precipitation, river flooding, and coastal hazards, and their associated economic impacts.

1. Introduction

Climate change due to global warming is expected to have major impacts on phenomena such as tropical cyclones (TCs), monsoons, precipitation, and seasonal storms. For example, average global TC precipitation rates and intensities are projected to increase in the late 21st century with medium confidence by the Intergovernmental Panel on Climate Change (IPCC) in the Special Report on the Ocean and Cryosphere in a Changing Climate (SROCC; IPCC, 2019). In addition, Working Group II (WGII) of the Fifth Assessment Report (IPCC-AR5) summarizes that climate change will exacerbate vulnerability at regional scales to extreme and impulsive physical processes and related natural hazards (IPCC 2013, 2014), such as heavy precipitation (e.g., Fischer and Knutti, 2016; Pfahl et al., 2017; Aalbers et al., 2018), river flooding (e.g., Hirabayashi et al., 2013; Arnell and Gosling, 2016), and storm surge (e.g., Lowe and Gregory, 2005; Lin et al., 2012).

As such, it is important to assess the impact of climate change on

natural hazards. However, this is still difficult on regional scales due to differences in scales between general circulation models (GCMs) and hazards, which are less than 10–500 km. While general impacts of climate change on natural hazards were discussed in the IPCC-AR5, the number of assessments with quantitative results on individual regional scales (e.g., Asia) are still limited. It is highly expected that climate change impacts on regional scales will feature prominently in upcoming or future IPCC reports, such as the Sixth Assessment Report (IPCC-AR6) or later.

1.1. Quantifying impacts of climate change on storm-related hazards

Climate change due to global warming is expected to greatly affect storm-related hazards such as TCs and other heavy precipitation events. The temporal and spatial scales of these phenomena range from $O(10 \text{ min})$ to $O(\text{days})$ and from $O(1 \text{ km})$ to $O(1000 \text{ km})$, respectively; in addition, the physical understanding to detect and attribute trends from

* Corresponding author.

E-mail addresses: mori.nobuhito.8a@kyoto-u.ac.jp (N. Mori), takemi@storm.dpri.kyoto-u.ac.jp (T. Takemi), tachikawa@hywr.kuciv.kyoto-u.ac.jp (Y. Tachikawa), tatano.hirokazu.7s@kyoto-u.ac.jp (H. Tatano), shimura.tomoya.2v@kyoto-u.ac.jp (T. Shimura), tanaka.tomohiro.7c@kyoto-u.ac.jp (T. Tanaka), fujimi@kumamoto-u.ac.jp (T. Fujimi), osakada.yukari.77v@st.kyoto-u.ac.jp (Y. Osakada), webb.adreanandrew.4c@kyoto-u.ac.jp (A. Webb), nakakita@hmd.dpri.kyoto-u.ac.jp (E. Nakakita).

<https://doi.org/10.1016/j.wace.2021.100309>

Received 12 September 2020; Received in revised form 25 November 2020; Accepted 26 January 2021

Available online 3 February 2021

2212-0947/© 2021 The Author(s).

Published by Elsevier B.V. This is an open access article under the CC BY-NC-ND license

(<http://creativecommons.org/licenses/by-nc-nd/4.0/>).

the phenomena are also different (Kunkel et al., 2013; Peterson et al., 2014). TCs in particular, are a key driver of natural disasters in East Asia. In order to assess the impact of climate change on TC-related hazards, it is critically important to quantitatively represent TC-induced heavy rainfalls using strong wind and pressure fields at local scales. However, in comparison with the larger global-climate-projection scale, these fields are sub-scale and generated locally. Therefore, dynamic and statistical impact assessments which use downscaling techniques are required to understand the long-term impacts of climate change on natural hazards. If extreme natural hazards become more frequent or dangerous in the future, it is necessary to consider their effects to prevent or at least reduce their impact on vulnerable areas. Additionally, it is also necessary to estimate the potential economic damages caused by climate change in order to properly understand the costs of adaptation.

Projecting future changes of many TC-related hazards and/or their potential economic impacts can be challenging due to the relatively small scale of the phenomena in a GCM and their low occurrence frequencies in any one particular area. The effects of model resolution on projected climatological features of TCs have been investigated in both atmosphere-only and coupled simulations. For example, Murakami and Sugi (2010) showed that resolutions of 60 km or finer (investigations ranging from 180 km to 20 km) are critical for projecting future changes in the occurrence frequencies of intense TCs in a joint atmospheric global circulation model (AGCM) by the Japan Meteorological Agency (JMA) and Meteorological Research Institute (MRI). Comparably, Roberts et al. (2020b) found that some 20–50 km resolution models from the Coupled Model Intercomparison Project (CMIP) Phase 6 (CMIP6) High Resolution Model Intercomparison Project (HighResMIP) are able to reproduce occurrence frequencies comparable to observations in coupled simulations as well. Despite improvements in resolution however, Roberts et al. (2020a) suggest that some single-model ensemble averages are still necessary to distinguish impacts from resolution and internal variability.

Quantifying climate uncertainties (i.e., signal-to-noise ratio) is important for projection-based impact assessments of extremes; correspondingly, understanding modeling uncertainties better is of key interest for climatological research. While potentially computationally expensive, the challenge of low occurrence frequencies can be overcome by using a large number of ensemble projections to analyze low occurrence frequency extremes. For instance, Yoshida et al. (2017) used variable ensemble member averages of a 60-km AGCM to analyze changes in the occurrence frequencies of intense TCs and found that uncertainty ranges decreased as the number of ensemble members increased (d4PDF dataset; see discussion below). Modeling uncertainties can also be estimated by increasing the number of ensembles in a single-model projection (Murphy et al., 2004), as well as by analyzing multi-model projections. In the latter, Roberts et al. (2020b) demonstrated how multi-model ensembles can be used to reduce uncertainties resulting from model physics and TC detection methods and found robust changes in TC activity in the Southern Hemisphere.

Several single-model large-ensemble datasets have been created to quantify uncertainty and increase modeling fidelity of weather phenomena under climate change. In a pioneering work by Kay et al. (2015), a single-model large-ensemble dataset was generated using the Community Earth System Model (CESM) in the United States; it covers a 180-year period (1920–2100) and consists of 30 projection members initialized with small atmospheric differences. The CESM ensemble dataset provides an internal climate variability of the ensemble-mean projection and has been used in several applications. For example, Hagos et al. (2016) analyzed the impact of global warming on atmospheric rivers making landfall in western North America. By considering the internal variability of the location of a subtropical jet and its associated extreme precipitation, they were able to quantify probabilistic changes in atmospheric rivers making landfall. In general, most large ensemble climate datasets use a global warming scenario that covers a period from the present to end-of-century. However, Maher et al. (2019)

recently created the Max Planck Institute Grand Ensemble in Germany which contains four future climate scenarios (and historic) with 100 members each. In the landmark study, the authors demonstrate how the multi-scenario large-ensemble dataset can be used to differentiate the forced signal from internal variability under anthropogenic warming.

A similar pioneering work on large climate projection ensembles has been conducted with extensive collaboration among climate research groups in Japan. The Database for Policy Decision-Making for Future Climate Change (d4PDF) is a mega-ensemble climate simulation dataset that was generated to overcome the difficulties of projecting future changes of TC-related hazards and economic impacts (Mizuta et al., 2017). The d4PDF dataset was designed to compare historic and future climate conditions at end of twenty-first century under the Representative Concentration Pathway (RCP) 8.5 scenario (RCP8.5) and consists of long-term ensemble projections (spanning 60 years each) at relatively high-resolution global (60 km) and regional (East Asia, downscaled to 20 km) scales using the AGCM MRI-AGCM 3.2H (Mizuta et al., 2012) and non-hydrostatic regional climate model (NHRCM) d4PDF-RCM (respectively). The historical climate conditions (global/regional: 100/50 ensembles, 6000/3000 years) cover the period 1951–2010 and are perturbed based on uncertainties in observed sea surface temperatures (SSTs). The future climate conditions (global and regional: 90 ensembles, 5400 years) are based on SST warming patterns from six CMIP5 models (selected to maximize geographical uncertainty) that have been perturbed and scaled such that global mean temperatures are +4 K from before the Industrial Revolution (c.a. 1850). In short, three main characteristics—(1) large number of ensembles of over 5000 years for both historical (global) and future climate conditions, (2) same prescribed phase of warming during the entire future climate condition (i.e., constant +4 K global mean temperature), and (3) combined use of an AGCM and NHRCM—make it possible to analyze low occurrence frequency events, including TCs in East Asia. In particular, the use of the same prescribed warming phase (for the future climate condition) is beneficial for analyzing extreme events since traditional extreme value analysis requires a stationary assumption. Many studies are now using the d4PDF dataset in impact assessments to directly estimate hazards with low occurrence probabilities and/or longer return periods of 100 years or more (e.g., Tanaka et al., 2018; Yang et al., 2018; Hatsuzuka and Sato, 2019); for a full review, see Ishii and Mori (2020).

1.2. Nationwide climate change projection, impact assessment, and adaptation programs

Around the world, national (and international) programs have been set up and commissioned to coordinate and evaluate climate change projections, impact assessments, and adaptation strategies. For example, two regions with robust efforts are the United States and Europe. Since 2000, the United States Global Change Research Program (USGCRP; 13 member interagency program initiated in 1989) has coordinated federal research to examine global changes and analyze societal implications in order to inform U.S. policy makers and the public. The USGCRP has released four National Climate Assessment (NCA) reports and have provided public access to the federal information products used for producing the reports. The latest report, NCA4 Volume II (USGCRP, 2018), summarizes the importance of global mitigation and regional adaptation efforts to minimize impacts on the public's physical, social, and economic well-being. In 2018, the European Environment Agency (EEA) and the European Topic Center on Climate Change Impacts, Vulnerability and Adaptation (ETC/CCA) coordinated the first systematic review of national assessments conducted by EU members. In addition, the European Climate Adaptation Platform, Climate-ADAPT, was set up in 2012 to help distribute climate change information and coordinate adaptation measures in Europe. The United Kingdom has also carried out a series of climate change projections known as UK Climate Projections 2009 and 2018 (UKCP09 and UKCP18, respectively) (Lowe et al., 2018). The latter, UKCP18, focuses on integrating the most

recent weather and climate observations and analyses (including data from the latest generation of international climate models) with results from the UK Met Office global and regional climate models. The UKCP18 climate projections provides probabilistic projections of relatively small, medium, and large regional-scale changes, as well as sub-seasonal and sub-monthly extremes across the United Kingdom. The UKCP18 also quantifies the impact of climate change on water resources, flood risk, coastal erosion risk, and forestry.

Turning our attention towards the Asia-Pacific, Australia has produced a national report in 2015 entitled, “Climate Change in Australia” (CCIA), led by the Commonwealth Scientific and Industrial Research Organisation (CSIRO) and the Bureau of Meteorology of Australia (BoM) (CSIRO and Bureau of Meteorology, 2015; 2020). The report largely focuses on impact and risk assessment; in particular, it aims to estimate risk from climate variability, especially those from extreme events—such as from heatwaves, frost, flood, cyclones, storm surges, tornadoes, and hail. The CCIA has identified relevant spatial and temporal scales for the impact assessment (from seasonal to hourly for the latter) and important characteristics (intensity, frequency and/or duration) of the weather event for the associated risk. In Asia, Taiwan has been conducting the Taiwan Climate Change Projection and Information Platform Project (TCCIP) since 2010 (Hsu et al., 2011). The TCCIP aims to build up climate change research and projection efforts, consolidate information, and provide data access and tools for users. There are three teams in the TCCIP project (from projection to adaptation) and Team 3 deals with seasonal precipitation and drought, and TC and TC-related river and coastal flooding. These examples of national programs indicate that a deeper integration of climate change projections and impact assessments have been occurring over the last few decades. A common strategy of these programs is how to integrate from a global projection to a regional impact assessment using ensemble and downscaling methods. Different regions have different climatological (e.g., drought, fire, flood, and wind risks), geological (e.g., coastal and inland vulnerabilities), and social characteristics (e.g., risk sharing and operational preferences); therefore, different methodologies are required for impact assessments and adaptation strategies.

1.3. History of climate change projection and impact assessment programs in Japan

The Kyoto Protocol (2008–2012), Doha Amendment (2012–2020), and Paris Agreement (2020–) are international agreements within the United Nations Framework Convention on Climate Change (UNFCCC) that are based on scientific consensus and aim to reduce greenhouse gas emissions (GHGE). Given the current observed signals and future uncertainty in climate change, both mitigation and adaptation measures are important. While mitigation measures must be implemented globally, adaptation measures can be implemented at regional or national levels. Therefore, many regions and countries have released regional adaptation plans that address the increasing risks from climate change (e.g., Australian National Climate Resilience and Adaptation Strategy, 2015; UK Climate Change Risk Assessment, 2016; Pan-Canadian Framework on Clean Growth and Climate Change, 2019).

During a Cabinet meeting in November 2015, the Japanese government approved the “National Plan for Adaptation to the Impact of Climate Change”, in order to minimize or avoid impacts of climate change and establish a sustainable society (<https://www.env.go.jp/en/headline/2258.html>). Since then several climate change-related programs have been initiated in Japan, such as the Social Implementation Program on Climate Change Adaptation Technology (SI-CAT; 2015–2020) by the Ministry of Education, Culture, Sports, Science and Technology (MEXT; Japan), and the Strategic Research on Global Mitigation and Local Adaptation to Climate Change (MiLAi; 2015–2020) by the Ministry of Environment (Japan). These programs have primarily focused on regional projection downscaling or adaptation. More recently, the Integrated Research Program for Advancing Climate

Models, known as the TOUGOU Program (2017–2022), was initiated by MEXT to advance climate change studies in East Asia and apply the results for the benefit of society (<http://www.jamstec.go.jp/tougou/>). The TOUGOU Program aims to achieve these goals through four cooperative groups, known as Themes A–D, and supports active development of (A) a coupled atmospheric and ocean GCM (AO-GCM; MIROC) model, (B) an earth system model, (C) a high resolution GCM/RCM, and (D) impact assessment models. In addition, each group focuses on addressing specific scientific and societal needs—(A) understanding climate change mechanisms, (B) understanding the carbon cycle, (C) providing projection data for impact assessments, and (D) conducting regional impact assessments—all the while challenging the program as a whole to develop state-of-the-art climate change projection datasets. The TOUGOU Program is the only Japanese program that is (1) supporting active development of a GCM and providing global projections for CMIP6 and related regional downscaling efforts, and (2) bridging the gap between seamless projections and impact assessments by increasing model resolution and the number of ensemble members.

The Integrated Hazard Prediction group, Theme D of the TOUGOU Program (TOUGOU-D), is focused on understanding how climate change will affect (a) TC, (b) precipitation, (c) river and coastal flood, and (d) geological hazards, using the latest climate projections from Themes A–C as well as CMIP5/6 projections. By utilizing these projections, TOUGOU-D aims to project how the severity of natural disasters will change over the next 100 years and reveal the scientific relationships between these disasters and climate change. This is primarily achieved through two approaches—first, quantifying probabilistic changes of climate change impacts (such as TCs, flooding, etc.), and second, assessing the maximum severity of such impacts using worst-case scenarios that consider extraordinary situations (such as mega-TCs). By conducting integrated hazard assessments, TOUGOU-D analyzes future changes of the hazards and their social impacts in order to provide essential information and the necessary methods for preparing for no-regret adaptation measures. There are several common aims and methodologies between the TOUGOU Program and other national climate programs; however, TOUGOU-D is mainly focused on extreme hazardous events caused by TCs and Baiu weather systems.

1.4. Overview of review

The nationwide TOUGOU program aims to achieve its research goals by gathering major relevant climate projection and impact assessment research groups in Japan and providing a platform for increased collaboration and synergy. Here, we summarize the latest studies from TOUGOU-D (written in English or Japanese), which covers all aspects of climate change impact assessments and adaptation strategies of natural hazards conducted in Japan. Since one of the goals of the TOUGOU program is to advance climate change research in East Asia, we have included studies that cover the greater region when possible (Section 5 in particular). However, due to manuscript length considerations, we have narrowed the scope on some topics that have distinct sub-regional characteristics (such as the East Asian monsoon); in addition, we focus on high-resolution regional projections and impact assessments here, which tend to be centered around Japan.

An overview of this manuscript is illustrated in Fig. 1. First, we review projected future changes of TC-related hazards (wind, precipitation), followed by Baiu-related hazards (precipitation). We then review projected future changes in river flood risk (and their associated economic costs) and coastal hazards (storm surges, storm waves). And finally, we review the economic impacts of mitigating some of these natural hazards (such as storm surges) under current conditions of social exposure and vulnerability.

2. Tropical cyclones

TCs typically develop in the Pacific (north and southwest), Atlantic

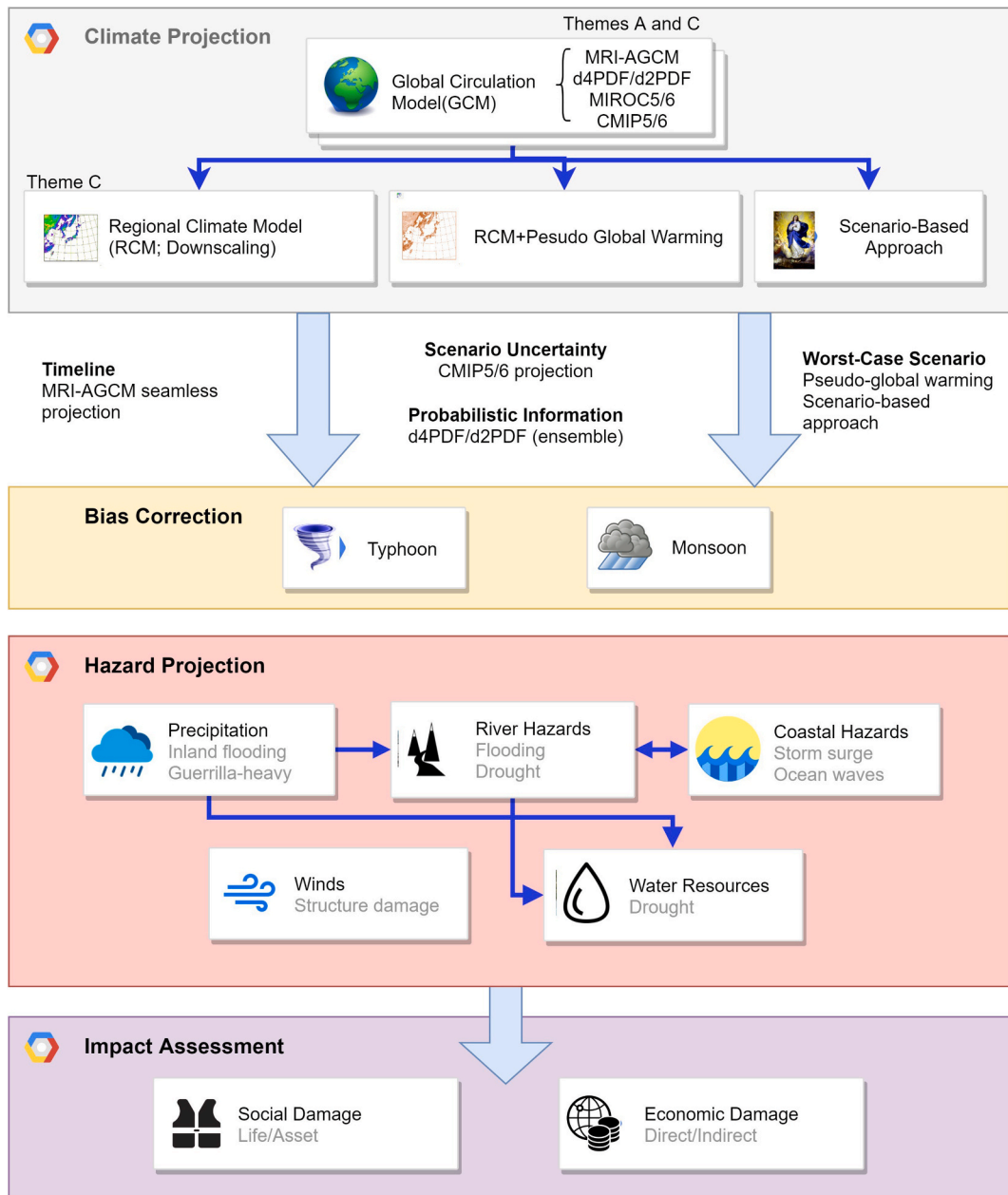


Fig. 1. Schematic view of research relations between different hazards and related impact assessment in this study.

(north), and Indian Oceans and are the most damaging storms in those regions. Therefore, forecasting and assessing the impacts of TCs are critically important for disaster prevention and mitigation. Since TCs are anticipated to become more destructive in a future warmer climate, the impacts of climate change on TCs should be quantified as precisely as possible. In the western North Pacific (WNP), a TC is called a typhoon. Large populations and significant economies in East and Southeast Asia are at risk from typhoon-related-hazards, and impacts from disasters are not just limited to these regions but affect other parts of the world. Therefore, we focus on the impacts of typhoons in this review.

2.1. TC hazard projection and impact assessment approach

Quantitative representations of TC-induced heavy rainfalls and strong winds at local scales are critically important for properly assessing TC-related hazards. For example, a slight difference in track path and intensity of a TC can result in large differences in the maximum

water level from a TC-induced storm surge in a bay (Mori et al., 2014). Therefore, downscaling TC hazards to local scales with a dynamical or a statistical approach is required to quantitatively represent the TC hazards. Common dynamical and statistical approaches used for downscaling are reviewed in detail in Mori and Takemi (2016), and both approaches have advantages and disadvantages that depend on the purposes of the investigation. The dynamical approach is straightforward and provides multivariable information; however, it is difficult to control phenomena within the location of interest (e.g., TC tracks), and the number of ensembles may be a limited because of the associated higher computational costs. The statistical approach on the other hand, can increase the number of events dramatically; however, a lack of physical processes can make it difficult to obtain multivariable information (e.g., relation between wind speed and precipitation) and there is a large dependence on model turning.

Here, we review studies that use the dynamical approach since it is advantageous to consider the meteorological settings of historical

extreme events (that led to severe disasters) when assessing TC hazards; impacts from these worst-case scenarios can then be quantified at local scales under realistic meteorological settings (Takemi et al., 2016c). In particular, we review the impacts of climate change on specific TC events that have been investigated using pseudo-global warming (PGW) experiments (Schär et al., 1996; Sato et al., 2007), which require climate perturbations and past meteorological analysis fields. The perturbations, or global warming increments, are generated by subtracting future and present climate states obtained from climate projection and long-term reanalysis datasets such as JRA-55 (Kobayashi et al., 2015), ERA5 (Hersbach et al., 2020), and others. A regional meteorological model is then used to conduct dynamical downscaling experiments for the present condition (reproduced from long-term reanalysis data), and for the future conditions, which are generated incrementally by adding the global warming increments to the analysis fields. Since most PGW experiments increment environmental variables (e.g., air temperature, humidity, and SST) that have historical records and reanalyses, it is not necessary to consider bias correction and is one of the main advantages of conducting PGW experiments (in comparison with conducting global climate projections that follow a particular GHGE scenario). Detailed procedures for conducting the PGW experiments can be found in Takemi et al. (2016c) and others (e.g., Gutmann et al., 2018).

In the studies reviewed here, the Weather Research and Forecasting (WRF) model (Skamarock et al., 2008) is used for all downscaling. In order to quantitatively reproduce TC intensities, high-resolution modeling of $O(1\text{ km})$ is necessary to capture the inner-core structure and rapid intensification process of a TC (Kanada et al., 2017a). Thus, dynamical downscaling on an $O(1\text{ km})$ resolution is also required in impact assessment studies. It should also be noted that in PGW experiments, it is important to keep the TC track unchanged both in the present and future climate conditions since a slight change in the TC track can result in large differences in TC impacts (as previously mentioned). Since a TC track is strongly controlled by the background steering flow, any changes to the steering flow will alter properties of the track. Even if the path of the TC is the same, the steering flow will affect the translation speed of the TC, and hence change the temporal location of the TC. Conversely, a difference in the location of a TC means that the steering flow for the TC was different (which led to a difference in the TC path). Therefore, in the dynamical downscaling approach, the steering flow for a TC should be kept unchanged as much as possible. To achieve this, a nudging technique is helpful for constraining the internal variability of the downscaled model.

In general, a nudging technique is implemented by adding a forcing term in the governing equation set, which is formulated as a tendency term that gradually nudges a selected term towards a targeted value during a specified time period (see Stauffer and Seaman, 1990; 1994). The nudging can be proportional to differences between simulations (numerical prediction model output) and either gridded analyses of observations (global nudging) (Stauffer and Seaman, 1990) or individual observations (local nudging) (Stauffer and Seaman, 1994). By nudging the selected term towards the targeted value, it is expected that the overall model prediction will be improved. Therefore, this general nudging technique has been widely used in mesoscale modeling and air-quality modeling (e.g. Otte, 2008). However, the technique is applied on a grid-scale level, and thus grid-scale noises (i.e., small-scale errors inherent in the numerical model analyses and observations) cannot be avoided.

In order to minimize the effects from such noises, a modified approach, the spectral nudging technique, was developed to remove unwanted small-scale features (Waldron et al., 1996). By retaining longer-wavelength spectral components and filtering out shorter-wavelength ones, this technique only nudges a selected term toward a targeted value having larger-scale features in a model domain (e.g., background steering flow) (von Storch, 2000). Therefore, this spectral nudging technique is particularly useful in weather and climate simulations since large-scale meteorological features from a GCM can be

incorporated into a RCM or a limited-area model (e.g. Lin et al., 2012; Tang et al., 2019). The effectiveness of the technique has been examined in a wide range of studies, including storm climatology over the North Atlantic (Weisse et al., 2005), cloud simulation (Meinke et al., 2006), and regional climate simulation over North America (Miguez-Macho et al., 2005). In addition to spectral nudging, the spectral boundary coupling (SBC) method (Kida et al., 1991) can also be used for downscaling. Here, only spatial fluctuations within the wavenumber space (representing the small-scale) are retained while large-scale features are directly replaced with the corresponding spatial-scale phenomena from a GCM. The SBC method was applied in a nonhydrostatic model to examine East Asian monsoon rainfall and was shown to perform well in reproducing long-term weather patterns and rainfall amounts (Yasunaga et al., 2005); it has also been implemented in several RCMs and used in subsequent regional climates studies (e.g., Sasaki et al., 2008; Kanada et al., 2012).

The spectral nudging technique has been implemented in the WRF model, and the option has been used widely in weather and climate simulations. Some examples applied to TCs near Japan include Takemi et al. (2016a) and Takemi (2018a; 2019), which successfully reproduced simulated TC tracks that are similar to actual tracks for typical (1) autumn-season TCs that land in Japan, (2) southern Pacific cyclones that develop from convective populations within a Madden-Julian oscillation, and (3) WNP and slow-moving summertime TCs that land on the Pacific side of Japan (respectively). By controlling the TC track under present and future climate conditions, it is possible to assess the impacts of TCs under different climate scenarios.

It is worth mentioning that in the context of the PGW experiments, any spectral nudging of the wind fields must be handled carefully. As discussed previously, the advantage of using the spectral nudging technique is that we are able to control the track of a TC and assess impacts of a specific TC on a specific area. If a slight change in the track occurs, the impact from a TC with a displaced track may be totally different than one with the same track. On the other hand, there may be possible disadvantages from using spectral nudging. If large-scale circulation fields (such as the position of monsoon-season stationary fronts, spatial patterns of the Pacific High or Tibetan High, etc.) are totally different between present and future climate conditions, large-scale circulation patterns in the PGW field will also be different from those in the present climate. Thus, the TC tracks in the present and future climates will be different, and therefore, the climate change impacts on TCs with similar tracks are not properly investigated. Furthermore, too much nudging may strongly affect the TC intensification process and affect the TC maximum intensity in turn, which will be regarded as a model artifact of the PGW experiment. As such, the purpose of the study must be considered carefully in order to determine the proper settings for spectral nudging.

Other issues with the PGW experiments include properly setting the SST fields and dealing with atmosphere-ocean coupling. To simplify, many PGW experiment studies often neglect ocean mixing caused by surface winds and atmosphere-ocean fluxes since it is not straightforward to determine appropriate ocean states under warmed climate conditions. Furthermore, there are still unknown aspects of atmosphere-ocean coupling, and coupling is a challenging problem even for numerical weather prediction of TCs. As such, uncoupled SST fields are often prescribed instead as boundary conditions for the atmosphere in order to avoid such modeling uncertainties. In the (majority of) PGW experiments reviewed here, this approach is taken and the SST global warming increments (between present and future climate conditions) are added to historic SST fields. However, limited concurrent studies have begun to investigate how atmosphere-ocean coupling can influence the development of TCs under global warming (e.g., Kanada et al., 2019). Indeed, numerous processes near the surface interface control enormous exchanges of heat and trace gases between the atmosphere and ocean. For instance, strong winds can entrain cold water masses beneath the mixed layer through vertical shear mixing, which in turn

will affect heat and water vapor fluxes. It is critically important to estimate these surface fluxes properly in order to reproduce TC intensities accurately (Emanuel 1986; Rotunno and Emanuel 1987; Bryan and Rotunno 2009; Miyamoto and Takemi 2010). As such, it is essential for future studies to further uncover the role that atmosphere-ocean coupling plays in changing TC intensity and structure in a warmed climate state.

2.2. TC impacts in Japan

A large number of studies have investigated the impacts of climate change on TCs, and a review of all the relevant studies in general falls outside the scope of this paper. However, there are several recent assessments by Knutson et al. (2019; 2020) that should be mentioned in order to infer climate change impacts on TCs over Japan. In the first assessment, Knutson et al. (2019) used historical observation data to assess detectable changes in TCs and concluded with a low-to-medium confidence that the observed poleward migration of the latitude of maximum intensity in the WNP is detectable (highly unlikely to occur from natural variability alone). In a second assessment, Knutson et al. (2020) used model projections to assess TC responses to future anthropogenic warming. The study indicates with higher levels of confidence that higher storm surge levels will occur (enhanced by sea level rise due to global warming), and that there will be an increase in TC-related precipitation, global-mean TC intensity, and proportion of very intense TCs; however, confidence levels are lower for basin or regional scale projections of TCs. Thus, there are a number of uncertainties in investigating and demonstrating climate impacts on TCs in Japan, not only for future projections but also for historical observations. In fact, the mean annual number of TCs in the WNP is about 26, while the number of TCs that land or approach the Japanese islands is only about 11. Such limited numbers make it difficult to conduct statistically robust impact assessments of climate change on TCs, especially at local scales. Hence, the number of samples is critically important for demonstrating TC impacts at such local scales, like areas within the Japanese islands.

For these reasons, the use of the d4PDF dataset is a breakthrough in impact assessment studies. For example, Yoshida et al. (2017) showed that the number of very intense TC developments increases over a broad area including the south of Japan in spite of an overall decrease in the total number of TC occurrences. However, the d4PDF dataset is not perfect since the horizontal resolution is not fully sufficient to resolve the internal structure of TCs. Therefore, there are still uncertainties in assessing local-scale impacts of climate change on TCs near Japan. Using observational data, Yamaguchi et al. (2020a) investigated the impacts on climate change on TCs during the past 40 years by focusing on TCs that approached the Tokyo area; they demonstrated that (a) the number of approaching TCs has increased and that (b) TC intensity has increased as translation speeds have decreased. While there are trends in the past climate variation due to both natural variability and global-warming, the study of Yamaguchi et al. (2020a) is regarded as a guide for understanding and revealing projected changes in TC impacts in future climates. Yamaguchi et al. (2020b) further examined the influence of climate change on TC translation speed in mid-latitudes; by comparing historical model simulations in the d4PDF dataset with and without observational global warming trends, the authors found that TC translation speeds in mid-latitudinal regions decrease with anthropogenic forcing, owing to both natural decadal climate variabilities and anthropogenic warming. In addition, it was shown that global warming in the future climate conditions of the d4PDF dataset leads to an increased number of slowly-moving TCs in autumn. If the translation speeds of a future TCs decrease, then the time durations of heavy rainfalls and strong winds are anticipated to increase, leading to harsher TC impacts locally.

In terms of the number of fatalities, Typhoon Vera (1959) (also known as the Isewan Typhoon) is the most devastating TC on record in modern Japan. Therefore, Typhoon Vera is regarded as a basis for a

worst-case TC scenario when considering climate change impacts. In Kanada et al. (2017a), a set of PGW experiments for Typhoon Vera were conducted using four non-hydrostatic models (with a horizontal 1 km resolution) in order to reveal robust responses of a Vera-class TC in a warmer climate condition; the authors found that all the models unanimously project an increase in the maximum intensity in the warmer climate by generating deeper and more intense updrafts in the eyewall. In addition, Takemi et al. (2016a) further showed that the intensity of Typhoon Vera is stronger in a warmer climate than in historical conditions (September 1959), not only at the time of maximum intensity but also at the time of landfall on the Pacific coastal side of Japan (Table 1). As TC intensity increases, the severity of local-scale rainfall and wind events are predicted to also increase.

The climate change impacts of a destructive, extreme-rain-producing TC have also been investigated with a horizontal 1 km resolution; Typhoon Talas (2011) was a slow-moving TC that brought a significant amount of rainfall, exceeding 2000 mm in total, over the Kii Peninsula (see Fig. 2) on the Pacific coastal side of Japan and caused widespread landslides as well as river flooding. Oku et al. (2014) generated a worst-case TC track for local-scale rainfalls over the Kii Peninsula by performing ensemble simulations of varying TC tracks using the potential vorticity inversion methodology (Ishikawa et al., 2013) and found that Talas' actual track is close to the worst-case track. Thus, Typhoon Talas is regarded as a worst-case TC scenario for extreme rainfall. Takemi (2019) conducted PGW experiments for Typhoon Talas and found that the extremes of the accumulated rainfalls over the Kii Peninsula are projected to be harsher in the future climate scenario, owing to a significant increase in precipitable water content (Fig. 3). It should be noted that the precipitable water content amounts to 100 mm, which is extremely large and would not appear in our current climate conditions. Therefore, as a common response to warmer climate conditions, analyses of Typhoon Vera (1959) and Talas (2011) indicate that rainfall and wind hazards on the Pacific side of Japan are projected to be harsher in the PGW condition.

TC impacts in northern Japan appear differently from those on the southern-facing Pacific side of Japan. Based on the study by Oku et al. (2010), Ito et al. (2016) examined Typhoon Songda (2004) under a PGW condition by focusing on the changes in winds over Hokkaido. When the TC moved northward and was located in northern Japan, the TC intensity was found to weaken rapidly and become weaker in the warmer condition than in historic (September 2004) conditions. Further examination of environmental factors such as SST, vertical shear, and meridional temperature gradient at upper levels, revealed that the meridional temperature gradient at the 500-hPa level was smaller in the warmer condition than in historic conditions, indicating a weaker baroclinicity under global warming. This weak baroclinicity makes environmental conditions unfavorable for extratropical transition and

Table 1

Maximum intensity of Typhoon Vera in the 1959 and PGW conditions. Intensity is indicated in terms of central surface pressure (hPa) and maximum surface wind (m s^{-1}) at the times of lifetime maximum intensity and landfall on the Pacific coastal side of Japan. Landfall is defined as the point when the typhoon passes the 33°N latitude line and AT denotes air temperature.

	At time of maximum intensity		
	1959 Condition	PGW Condition	
Added variables	N/A	SST, AT	SST
Central pressure (hPa)	899.5–909.0	879.4–898.1	859.7–876.8
Maximum wind (m s^{-1})	55.4–61.8	64.6–66.5	71.1–73.3
	At time of landfall		
	1959 Condition	PGW Condition	
Added variables	N/A	SST, AT	SST
Central pressure (hPa)	926.2–932.7	912.7–929.5	887.8–892.4
Maximum wind (m s^{-1})	46.4–50.4	49.8–55.1	58.1–61.1

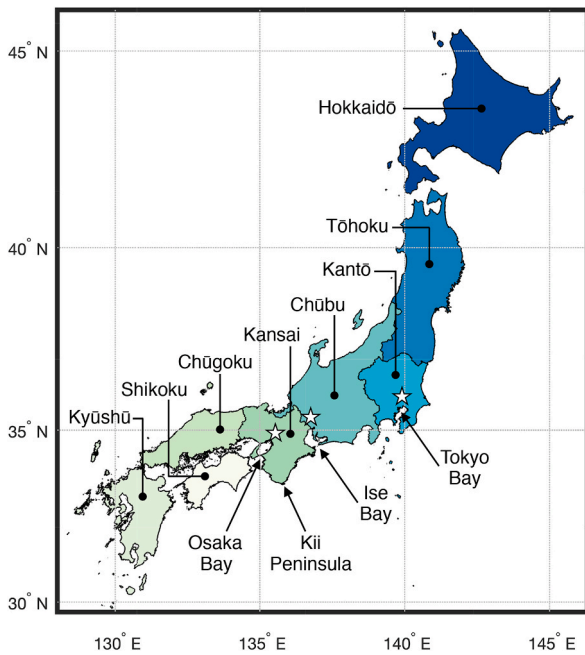


Fig. 2. Regions and locations discussed in study.

re-intensification, which in turn reduces the severity of TC winds in northern Japan. Thus, wind hazards over Hokkaido, in an ensemble-mean sense, become less severe under the PGW condition, leading to a reduced impact on forests in Hokkaido from TC-induced winds (Takano et al., 2016; Morimoto et al., 2019). A reduction of ensemble-mean winds in the northern part of Japan were also found in a similar analysis of Typhoon Mireille (1991) (Takemi et al., 2016b); however, maximum wind speeds during the TC passage become stronger in the warmed climate condition (versus the 1991 condition) in both the southern and northern parts.

Interestingly, climate change impacts on TC rainfalls in northern Japan are contrary to those on TC winds. Nayak and Takemi (2019a; 2019b; 2020a) investigated the influences of global warming on TC hazards in this region by conducting PGW experiments for Typhoons Chanthu, Mindulle, Lionrock, and Kompasu, which made landfalls in Hokkaido and Tohoku (respectively; see Fig. 2) and caused heavy rainfalls during August 2016. While the amount of rainfall is projected to increase in northern Japan under a warmer climate condition, wind speed responses to the warmer climate condition indicate a mixed feature. Kanada et al. (2017b) and Kanada et al. (2019) investigated TC-related rainfall in eastern Hokkaido by conducting PGW experiments with a horizontal 1 km resolution for three TCs that made landfall in August 2016. Their projections indicate that the frequency of strong rainfall will increase but the frequency of weak rainfall will decrease; a larger amount of convective available potential energy in the PGW condition is shown to contribute to stronger updrafts, and hence stronger rainfall in the TC core regions. In a follow-up study (non-PGW experiment), Kanada et al. (2020) used three-dimensional fields from the d4PDF dataset as initial and boundary conditions for a regional

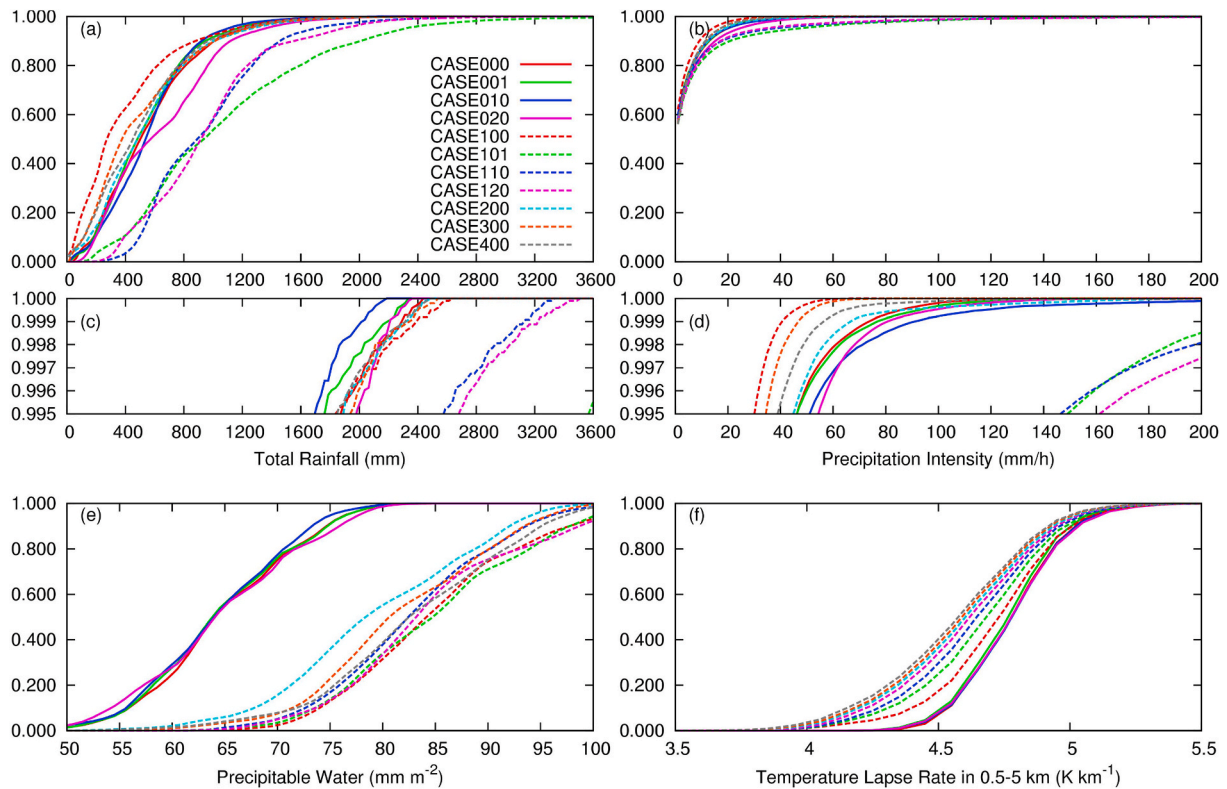


Fig. 3. Cumulative frequency distribution of rainfall and atmospheric conditions for Typhoon Talas (2011). Top row shows (a) total and (b) hourly rainfall for land grid points over the Kii Peninsula with (c,d) closeups of their respective extremes underneath. Bottom row shows (e) precipitable water vapor and (f) temperature lapse rate in the 0.5–5 km layer computed over the ocean upstream of the Kii Peninsula (adapted from Takemi, 2019).

model and directly downscaled select TCs that made landfall in eastern Hokkaido during the +4 K future climate conditions. They analyzed projected changes in the TCs and found that unusually intense TCs with extreme winds and heavy rainfalls can develop in midlatitudes by retaining their axisymmetric TC structures under conditions of higher SST, higher surface water vapor, and lower baroclinicity. This suggests that extreme TCs will shift northward in the Northern Hemisphere (while retaining their intensity) when unfavorable conditions for TC development are negligible.

The impacts of climate change may also affect the tropospheric temperature lapse rate, depending on the SST conditions under an assumed global warming scenario and the resulting radiative-convective equilibrium state. Since static stability is projected to increase as SSTs rise under future climate conditions, it may not be easy to separate the effects from increasing SSTs and decreasing lapse rates. Although atmospheric stratification and SST are correlated, the relations between them are nonlinear and depend on the AO-GCM used (e.g., Mori et al., 2021). Several studies have analyzed these relations under climate change; a useful approach for investigating the effects of changes to stability, is to examine the question, how TCs respond to changes in environmental conditions (including static stability), as an initial value problem. Using GCM experiments with varying temperature lapse rates, Shen et al. (2000) investigated the effects of atmospheric stability on TC intensity and showed that the simulated TCs intensify in a more unstable atmosphere. Likewise, Hill and Lackmann (2011) examined the effects of climate change on the structure of TCs by conducting sensitivity experiments with a regional model (WRF) using projections from multiple GCMs with changes in resolution, physical processes, and future climate conditions. They showed that TC intensity increases in almost all future conditions irrespective of resolution or physical process. In contrast, Kanada et al. (2017a) showed that Typhoon Vera would intensify under future conditions with the RCP8.5 scenario; this intensification occurs in spite of a more stable troposphere, mainly because of an increase in water vapor content and SST. They also showed that updrafts within the eyewall of Typhoon Vera would intensify and reach higher levels under the same future conditions. Thus, some studies have shown that a stabilized atmosphere suppresses excessive development of TCs despite increases in SST (Hill and Lackmann, 2011), while others have suggested that a tropospheric destabilization—caused by increases in water vapor content and surface moisture enthalpy flux—enhances secondary circulation of TCs (Kanada et al., 2017a). To help clarify, Takemi and Yamasaki (2020) conducted idealized numerical experiments with an axisymmetric non-hydrostatic model and found that TC intensity increases are 1.3–1.9 m s^{-1} per 1% change of the lapse rate and 0.1–0.5 m s^{-1} per 1% change of the tropopause height. These results indicate that the intensity of simulated TCs change more rapidly with an increase in temperature lapse rate than with an increase in tropopause height. Considering that a change in lapse rate has a significant negative impact on TC intensity, any intensification of TC strength must coincide from a significant increase in SST and moisture content. Takemi and Yamasaki (2020) have also suggested that more stable conditions found in warmed climate conditions will serve as a limiting factor to prevent extreme intensification of TCs under future climate change.

In this way, the impacts of global warming on landfalling or approaching TCs in Japan have been shown to appear differently, depending on the latitudinal location. From an impact assessment point-of-view, the hazard information should be downscaled to local-scales and furthermore, city-scales. In response to severe damage (caused by extreme winds) that occurred in cities during Typhoon Jebi (2018), Takemi et al. (2019) examined quantitative representations of strong winds within a real urban district of Osaka City by combining results from the WRF model with a large eddy simulation (LES) model with an $O(100 \text{ m})$ resolution developed by Yoshida et al. (2018). The authors found that the variability of building height and distribution

strongly affects the turbulent airflows within the urban district and thereby determines the local-scale characteristics of maximum instantaneous winds (Fig. 4), which were previously identified in idealized simulation settings by Yoshida and Takemi (2018). A next step will be to implement the changes in these meteorological forcings into city-scale models for climate change assessments. Because regional climate model (RCM) outputs are used as boundary conditions for city-scale LES models, the impacts of climate change on meteorological forcings are incorporated into the boundary conditions as changes in wind and thermal stratification. Such wind and stability changes are considered to affect strong winds at the surface level and within the urban canopy through changes in the downward transport of high momentum above the urban roughness sublayer. With this approach, a quantitative assessment of strong winds at the surface level and within the urban canopy is practicable, and hence useful for devising strategies and measures for climate change adaptation.

3. Baiu and precipitation

Baiu (known similarly as Meiyu in China and Changma in Korea) is a regional rainy period in Japan during late spring and early summer that is caused by persistent precipitation along a stationary front (rain belt) extending over eastern China, East China Sea, Korean Peninsula, and Japanese islands. Rainfall during the Baiu season sometimes becomes severe and generates disasters such as flooding and landslides on local scales and even on larger basin-wide scales. Alongside this, short-lived intense rainfalls are also generated by rapidly developing, isolated thunderstorms known commonly in Japan as ‘Guerrilla-heavy rainfall’ or ‘Guerrilla rainstorms’ (former term adopted here; e.g., Kawabata et al., 2011; Nakakita et al., 2017b). These individual thunderstorms have particularly short lifetimes and as such, hazardous flash floods are prone to occur; in addition to atmospheric phenomena, the term ‘Guerrilla-heavy rainfall’ is often used to refer to the associated disasters. Therefore, Baiu frontal activities (i.e., extreme rainfalls) and Guerrilla-heavy rainfall (i.e., isolated thunderstorms) are some of the major meteorological hazards in Japan. Here we overview some of the recent findings on the impacts of global warming on hazardous rainfall.

3.1. Baiu precipitation and localized heavy rainfall

Baiu precipitation is a major producer of extreme rainfall events in East Asia. Because of its societal impacts, Baiu precipitation has been studied not only from a weather forecasting viewpoint but also from a climate projection one. Therefore, a number of studies have examined the effects of warmed climate conditions on Baiu precipitation and background circulation features using AGCMs (e.g., Kitoh and

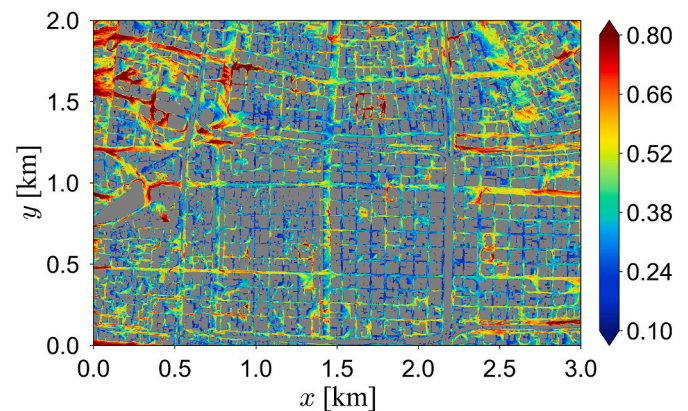


Fig. 4. Spatial distribution of maximum instantaneous wind speed at 10-m height. Results are from a LES analysis of airflows in an urban district of Osaka City (adapted from Takemi et al., 2019).

Uchiyama, 2006; Kusunoki et al., 2006; Yasunaga et al., 2006; Kusunoki et al., 2011; Hirahara et al., 2012) and RCMs (e.g., Kawase et al., 2009; Kanada et al., 2012). For example, climate change impacts on atmospheric circulations during the Baiu period over Japan and the surrounding regions were investigated by Okada et al. (2017). They used simulation data from MRI-AGCM 3.2S (20-km-mesh; Mizuta et al., 2012) for present-day (1979–2003) and future (2075–2099) climates under the RCP8.5 scenario; the future climate projection dataset consists of four ensembles driven by different SST types (Mizuta et al., 2014). The authors revealed that future changes of atmospheric circulation during June have a robust commonality among all the future climate simulations (i.e., different SST conditions), while future changes during July and August exhibit different patterns depending on the SST pattern. Thus, future changes of Baiu precipitation during the latter months are strongly controlled by those different circulation features.

Several groups have investigated future changes of extreme rainfall events during the Baiu season under a global warming scenario by using a 5-km-mesh NHRCM (NHRCM05) forced with an AGCM and the Special Report on Emissions Scenario (SRES) A1B. By analyzing characteristics of precipitation, Kanada et al. (2012) showed that the occurrence frequency of heavy rainfall will increase in early July of the realized future climate. Furthermore, Nakakita et al. (2012) showed that the occurrence frequency of Baiu localized extreme rainfall will also increase and was the first study to uniquely identify localized extreme rainfall events. Since the NHRCM05 has a spatio-temporal resolution sufficiently high enough to represent localized events (with spatial scales of $O(10)\sim O(100)$ km and temporal scales of several hours), they were able to manually identified events from the NHRCM05 precipitation distribution output based on rainfall amount criteria (such as 50 mm/h), as if they were from a weather radar image. If it was not possible to determine whether an event was a Baiu-type (belt-shaped) extreme rainfall event using rainfall amount criteria alone, the location of the Baiu front was checked using the north-south gradient of equivalent potential temperature on the surface.

Based on work in Nakakita et al. (2012), Nakakita et al. (2016) connected extreme rainfall with atmospheric patterns in d4PDF and showed that the occurrence frequency of specific atmospheric patterns that are prone to extreme rainfall will also increase in the future. Characteristics of future changes of atmospheric circulation during Baiu season had been clarified in previous studies (Ohba and Sugimoto, 2019; Okada et al., 2017), however Nakakita et al. (2016) was the first study to connect extreme rainfall events identified directly from an NHRCM05 with atmospheric circulation patterns. Since this study, a series of other climate change studies have begun to investigate the relationships between extreme events and atmospheric characteristics. For example,

Nakakita and Osakada (2018) and Osakada and Nakakita (2018a) analyzed four ensemble members of NHRCM05 under the newer RCP8.5 scenario and showed that the occurrence frequency of extreme rainfall will increase in all future ensemble members. In addition, by analyzing future changes of the corresponding atmospheric patterns, they were able to reveal the reasons why Baiu extreme events are not likely to increase significantly on the Pacific side. In a following study, Osakada and Nakakita (2018b) uncovered an increasing future trend in the accumulated amount of extreme rainfall (Fig. 5) using the same model. To investigate further, Osakada and Nakakita (2020) conducted a PGW experiment based on MRI-AGCM 3.2S climate data (under the RCP8.5 scenario) using a cloud resolving numerical model with a horizontal 500 m resolution. In addition to the expected linear thermodynamical effect caused by increased water vapor in the future climate condition, they found that there is also a non-linear dynamical effect that strengthens the formation process that organizes and maintains the rain-band system. These studies on extreme rainfall have ushered in a new phase of projecting future changes quantitatively.

The climate change impacts on extreme events due to Guerrilla-heavy rainfall (i.e., rapidly developing isolated thunderstorms) have also been investigated in Japan. These rainstorms have a smaller spatio-temporal scale than the Baiu localized extreme rainfall. It has long been thought that it is difficult to estimate future changes of Guerrilla-heavy rainfall because even a RCM with a 5-km-mesh cannot resolve the smaller scales necessary to analyze the rainstorms. However, Nakakita et al. (2017a) realized that the future projections of Guerrilla-heavy rainfall could be generated by analyzing multi-polarimetric weather radar and NHRCM05 data together. First, they converted radar information (for 4 years for the month of August) with a 250-m-mesh and 1-min-average to a 5-km-mesh and 30-min-average (using a spatial moving and regional average, and 30-min time integration) in order to make comparisons with the NHRCM05. They then clarified how the rain rate or spatial area of the Guerrilla-heavy rainfall should be represented in the precipitation distribution of the NHRCM05, by using the converted radar data to define criteria (a tuned rainfall intensity threshold) for extracting Guerrilla-heavy rainfall events and then manually identifying events based on the criteria in the NHRCM05 data (Nakakita et al., 2018b). This was also the first study to estimate future changes of the smaller scale Guerrilla-heavy rainfall, and as a result, they found an increasing trend in the occurrence frequency during August around the Kansai region of Japan (Fig. 6).

In another study, Nakakita et al. (2018a) analyzed the competing forces of two main global warming effects—atmospheric stabilization caused by a decrease in the temperature lapse rate and destabilization caused by an increase in the lower-level water vapor and revealed that the effect of lower-level water vapor increasing surpasses

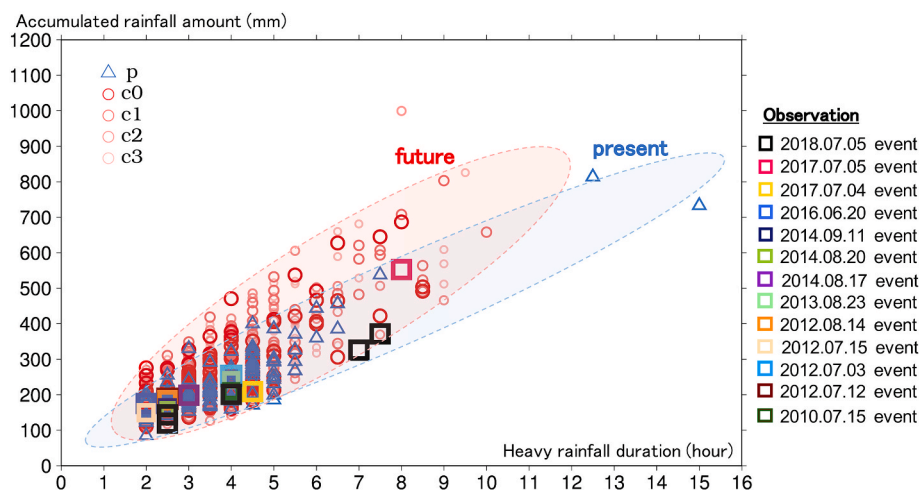


Fig. 5. Future changes of Baiu extreme rainfall (over 50 mm/h) in terms of duration and accumulated amount (during the duration). Shown are events projected by the NHRCM05 future (red circles) and present (blue triangles) climate experiments (20-years each). Individual ensemble members (c0, c1, c2 and c3) of the future experiments are distinguished with differing opacity. SST patterns in c0 and c2 are similar to the observed interannual variation pattern in ENSO. The SST pattern in c1 has opposite characteristics of c2, while c3 has larger warming in the WNP. Past real events picked up from multi-polarimetric weather radar are denoted with colored squares (adapted from Osakada and Nakakita, 2018b). (For interpretation of the references to color in this figure legend, the reader is referred to the Web version of this article.)

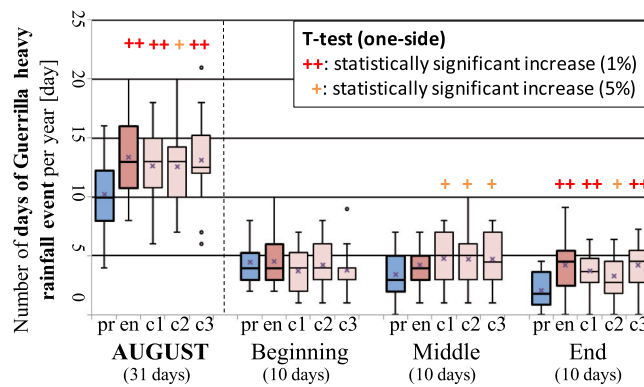


Fig. 6. Whisker plot showing the future change of the number of days in which Guerrilla-heavy rainfall events occur per year in August projected by the NHRCM05 climate experiments (for 20-years). The 1% and 5% statistically significant increases are denoted with symbols ++ and + (respectively). Future experiments use the same ensemble members (with different SST patterns) as in Fig. 5, with ‘en’ referring to ‘c0’ (adapted from Nakakita et al., 2017a).

mid-atmospheric warming, which leads to total atmospheric destabilization and can be the cause of increased Guerrilla-heavy rainfall. Moreover, by investigating the relationship between the Showalter stability index (SSI) and the occurrence frequency of Guerrilla-heavy rainfall, they were able to show importantly that (1) the SSI value can be used to estimate whether Guerrilla heavy rainfall will occur or not, and (2) the SSI threshold for judgement of atmospheric stability (i.e., whether Guerrilla heavy rainfall will occur or not) will not change in the future climate. As for future work of both the Baiu localized extreme rainfall and the Guerilla-heavy rainfall, it is necessary to further clarify the physical mechanisms that can increase the extreme rainfall occurrence frequency and intensify the rain rate, and to estimate quantitatively how much the rain rate or the accumulated amount of rainfall will increase in the future.

3.2. Recent observed extreme precipitation and its relation to climate change

During the warm season in Japan, quasi-stationary, band-shaped, precipitating systems often develop and sometimes lead to heavy and/or intense rainfalls. Unuma and Takemi (2016a) statistically analyzed the characteristics of such quasi-stationary precipitating systems and their environmental properties, and found that higher instability, larger amount of water vapor content, and middle-level high humidity are critically important in determining the intensity of the quasi-stationary precipitating systems. Among these precipitating systems, Unuma and Takemi (2016b) demonstrated that most have a linearly organized shape. Using radar and rain-gauge precipitation data, Hirockawa et al. (2020) developed a method to objectively identify heavy rainfall areas within mesoscale convective systems (MCSs); they found that the heavy rainfalls frequently occur on the Pacific sides of eastern and western Japan, with 60% of those observed to be in association with stationary fronts and tropical cyclones. By examining the morphological features, they showed that most of the linear-shaped rainfall areas are generated by elongated, stagnating MCSs. Furthermore, Kato (2020) reviewed the general characteristics of the quasi-stationary band-shaped precipitating systems (called *senjo-kousuitai* in Japanese) and statistically constructed favorable occurrence criteria from the environmental conditions.

In recent years, Japan has faced a number of extremely heavy rainfalls. Two cases among them, occurred in northern Kyushu in July 2017 and in western and central Japan in July 2018 and caused serious damages. Unuma and Takemi, 2021 examined the morphological characteristics of the cases, using an updated version of the automatic MCS detection algorithm from Unuma and Takemi (2016a), and demonstrated that the contribution from stronger rains (due to organized MCSs having areas of 200 km²) plays a major role in regions with a

significant amount of rainfall during the heavy rainfall events. To quantitatively assess the impacts of such extreme rainfalls, it is important to accurately reproduce rainfall amounts through the use of dynamical downscaling experiments (Takemi et al., 2016c) and multi-model approaches (Nayak et al., 2018). As clearly indicated in Takemi (2018b) and others, downscaling enables better reproduction of complex and complicated features due to topography, which has a positive impact on the quantitative representation of rainfall.

Nayak and Takemi (2020b) conducted PGW experiments for the 2017 and 2018 cases and found that the frequency and intensity of (averaged) extremely heavy precipitations during these events are higher under the PGW conditions. According to the Clausius-Clapeyron (CC) relationship, water vapor content increases by $\sim 7\% \text{ }^\circ\text{C}^{-1}$ under typical atmospheric conditions. While precipitation does not occur simply from condensation of water vapor (other mechanisms such as cyclonic motion, convection, and complex microphysical processes play critical roles), similar relationships between increasing rainfall rates and temperature can be found. In this context, the authors examined differences in the rainfall intensity further by comparing rates of increase with the CC relationship and found that the rate of increase for extreme rainfall intensity (on an hourly basis) is $\sim 3\% \text{ }^\circ\text{C}^{-1}$ in the present climate and is anticipated to rise to $\sim 3.5\% \text{ }^\circ\text{C}^{-1}$ under future climate conditions. The increases in precipitation intensity and CC scaling in future warmer climate conditions are attributed to (1) decreases in the temperature lapse rate and (2) increases in atmospheric water vapor and atmospheric energy, leading to the formation of more precipitation under the PGW conditions.

4. River flood risk

The d4PDF dataset is useful for detecting future changes in the frequency of the largest class of floods, as well as the resulting flood damages. However, the reliability of the results depends on the reproducibility of extreme rainfall against historical events. This section reviews the latest extreme flood disaster assessments that uses output from the regional d4PDF product (downscaled to 20 km), starting with (1) an evaluation of extreme rainfall in the d4PDF historic experiments compared with observed rainfall over Japan; (2) followed by an analysis of future changes of river discharge in highly urbanized basins (Arakawa River, Shonai River, and Yodo River basins) where the d4PDF extreme rainfall had a small bias; and (3) finally an assessment of future changes in economic flood risk in the Yodo River basin, Japan.

4.1. Bias characteristics of extreme rainfall in d4PDF over Japan

Recent studies have evaluated the ability of d4PDF to reproduce the annual maximum basin-averaged rainfall in Japan (e.g., Tachikawa

et al., 2017; Hoshino and Yamada, 2018). For example, Hoshino and Yamada (2018) compared the means and variances of annual maximum daily and 3-day basin-averaged rainfall over 109 class-A rivers in Japan in d4PDF with the observational dataset APHRODITE (Yatagai et al., 2012) and was the first study to quantify extreme rainfall biases in d4PDF with observational data covering all of Japan. However, the target rainfall durations were fixed 1–3 day(s) longer than the design rainfall durations in some river basins and may have also missed heavy rainfall events that spanned successive days (i.e., occurring near midnight).

In a following study, Tanaka et al. (2019) analyzed the characteristics of the extreme rainfall biases in d4PDF by comparing the probability distribution of annual maximum basin-averaged rainfall within the design rainfall duration in the (d4PDF) historical experiments with hourly data from the observational dataset Radar AMeDAS Rainfall (RAR) for the same 109 class-A rivers. The differences between the two distributions were statistically examined using the two-sample Kolmogorov-Smirnov (K-S) test and the p-values for all of the rivers are mapped in Fig. 7a. At a 5% significance level, d4PDF matches well with RAR in many river basins overall, while the null hypothesis is rejected for many rivers in the southern part of Japan. These areas have similar climate characteristics in that, extreme rainfall is mainly generated by TCs. These areas are also mostly covered by small river catchments and it was postulated that the biases might be attributable to an insufficient spatial resolution in the d4PDF. This possibility was examined by analyzing the relation between p-values and catchment area (Fig. 7b) and the results show that larger river basins have a larger p-value, indicating a dependence of d4PDF on the spatial scale of the target area. The smaller rivers on the other hand, show varying and not necessarily low p-values; therefore, the bias detected in extreme rainfall in the southern part of Japan is assumed to be regional, which might be related to the behavior of TCs in the AGCM and NHRCM used for d4PDF.

4.2. Future changes of the largest class river discharges in three highly urbanized river basins in Japan

Flood defenses for highly urbanized rivers are designed based on factors such as the frequency of extreme rainfall events and their resulting discharges; changes (in these factors) can be detected using long-term projection datasets such as d4PDF. In one such study, Tachikawa et al. (2017) analyzed the future changes of the probability distributions of extreme rainfall events and floods using a hydrological model with $O(100\text{ m})$ resolution and forced with d4PDF; in addition, they also analyzed the magnitudes of the largest class of floods, equivalent to a 1000-year flood. Three basins—the Arakawa River (2940 km²), Shonai River (1010 km²), and Yodo River (8240 km²)

basins—were studied in the Kanto, Chubu, and Kansai regions of Japan (respectively), which affect over 2 million people (see Fig. 7 for locations). The authors found that (i) in the target basins fortunately, the frequency distributions of annual maximum 24-h rainfall for the d4PDF historical experiment match well with the observed data, with p-values of 0.051, 0.053, and 0.121 for the two-sample K-S test for the Ara River, Shonai River, and Yodo River basins (respectively; see Fig. 8 in Tachikawa et al., 2017 for non-exceedance probability plots of each basin). In addition, the authors found that (ii) the 200-year annual maximum 24-h rainfall for the d4PDF future experiment is 1.3–1.4 times larger than the historic experiment (Fig. 8) and likewise, the annual maximum river discharge is 1.5–1.7 times larger (Fig. 9), and (iii) the 200-year annual maximum 24-h rainfall for the d4PDF future experiment is equivalent to the 900-year rainfall in the historic experiment. It should be noted that the study did not examine the simulated river discharge bias since observed discharge data is limited and statistical characteristics may be affected by river basin development; however, the simulated discharges (with a design return period of 200 years) for the historical experiment (7611 m³/s, 5975 m³/s, and 10,100 m³/s for the Arakawa River, Shonai River, and Yodo River basins, respectively) are consistent with the actual design values (7000 m³/s, 4400 m³/s, and 12,000 m³/s, likewise) (Ministry of Land, Infrastructure, Transportation and Tourism; http://www.mlit.go.jp/river/basic_info/jigyo_keikaku/gaiyou/seibi). And finally, the study revealed that the (iv) rainfall patterns that cause the largest-class floods simulated by d4PDF match well with one of the largest historical floods for the three basins. A similar study targeting the Nagara River basin (see Fig. 7 for location) was performed by Harada et al. (2018) and shows that future river discharges will increase by 1.33 times under the d4PDF future experiment. Future studies covering other river basins will clarify further the characteristics of future flood discharges in Japan.

4.3. Economic flood risk assessment: a case study in Yodo River, Japan

Quantifying the future change in flood risk based on projections of extreme rainfall is in high demand; however, the variability of the quantified flood risk is normally quite high and it is also important to measure the range of uncertainty. In Tanaka et al. (2016), a new method was proposed to develop flood risk curves that included impacts from the spatial-temporal rainfall variability. This method, Analytically Derived Flood Risk Curve (ADFRC), uses the probability distribution of annual maximum basin-averaged rainfall and was validated using historical flood records for the Yura River basin in Japan. By combining one ensemble of climate simulation data with the ADFRC, one flood risk curve could be obtained. In a follow-up study, Tanaka et al. (2018)

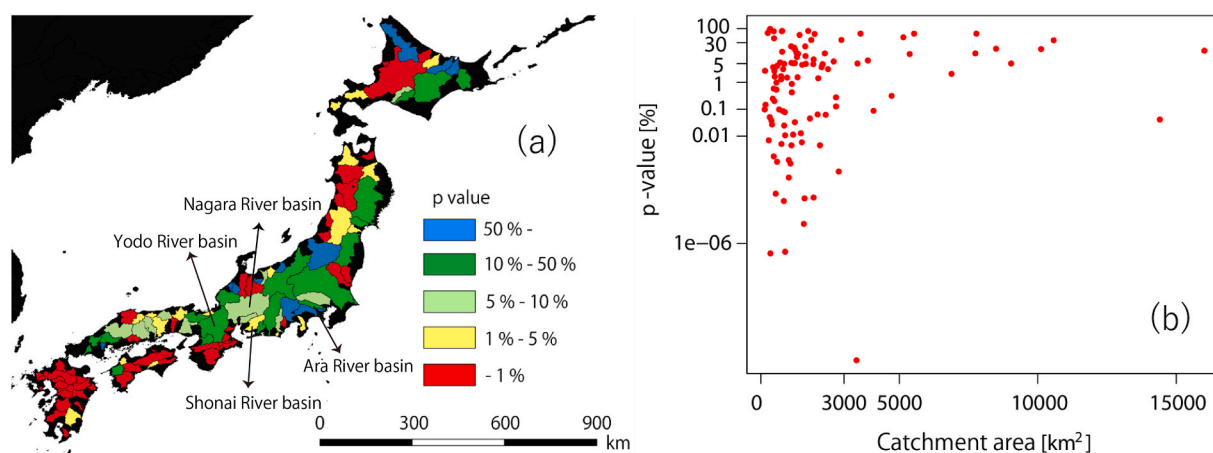


Fig. 7. Two-sample K-S test for annual max basin-averaged rainfall over Japan between d4PDF and RAR. Left (a) shows map of p-values for all 109 Class-A rivers in Japan; right (b) shows relation between p-value and catchment area for each river (adapted from Tanaka et al., 2019).

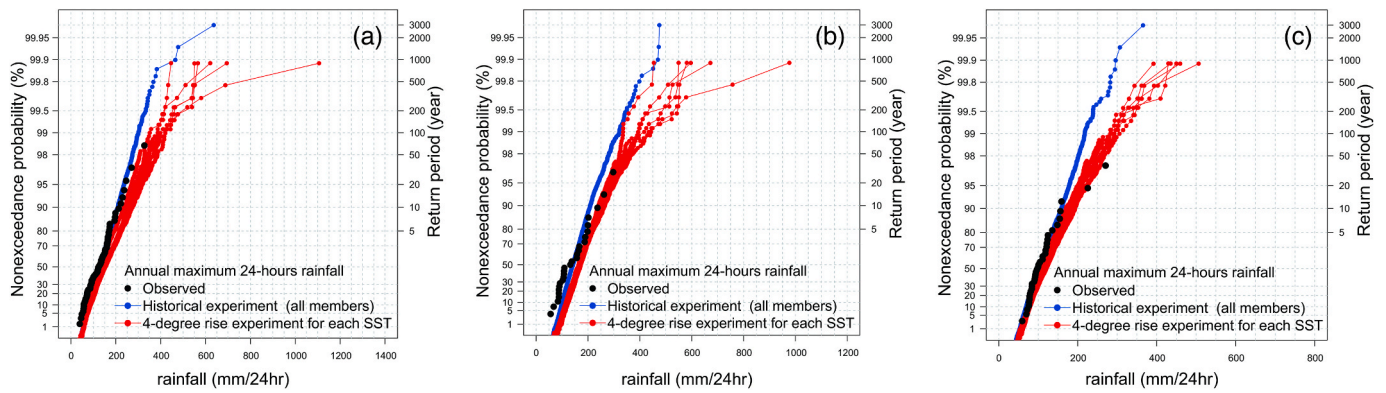


Fig. 8. Probabilities of annual maximum 24-h rainfall for observed and d4PDF historical and future experiments for the (a) Arakawa River, (b) Shonai River, and (c) Yodo River basins. The 200-year annual maximum 24-h rainfall for the d4PDF future experiment (red) is 1.3–1.4 times larger than historical experiment (blue) (adapted from Tachikawa et al., 2017). (For interpretation of the references to color in this figure legend, the reader is referred to the Web version of this article.)

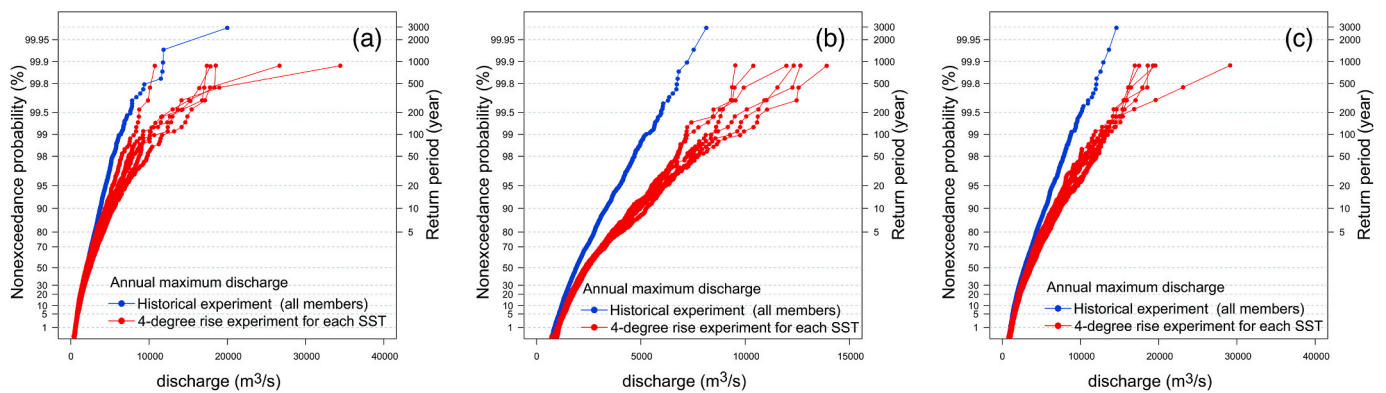


Fig. 9. Same as Fig. 8 but for annual maximum river discharge. The 200-year annual maximum river discharge for the d4PDF future experiment (red) is 1.5–1.7 times larger than the historic experiment (blue) (adapted from Tachikawa et al., 2017). (For interpretation of the references to color in this figure legend, the reader is referred to the Web version of this article.)

proposed using this idea with d4PDF and derived flood risk curves for each of the 50 historic and 90 future ensemble experiments spanning 60 years, using the Yodo River basin in Japan as a case study.

The derived flood risk curves in the historic experiment are shown in Fig. 10a. The authors found that flood damages with the same quantile vary more largely with larger return periods. Interestingly, a histogram

of the exceedance probability can be generated for a particular flood damage, as shown in Fig. 10b for 800 billion Japanese yen. Here, the histogram has a long tail (affected by the extreme rainfall) and the exceedance probability could be as high as 0.01, even though many members (including the combined case of using all members) are around 0.0015. In another study, Shimizu et al. (2019) analyzed future changes

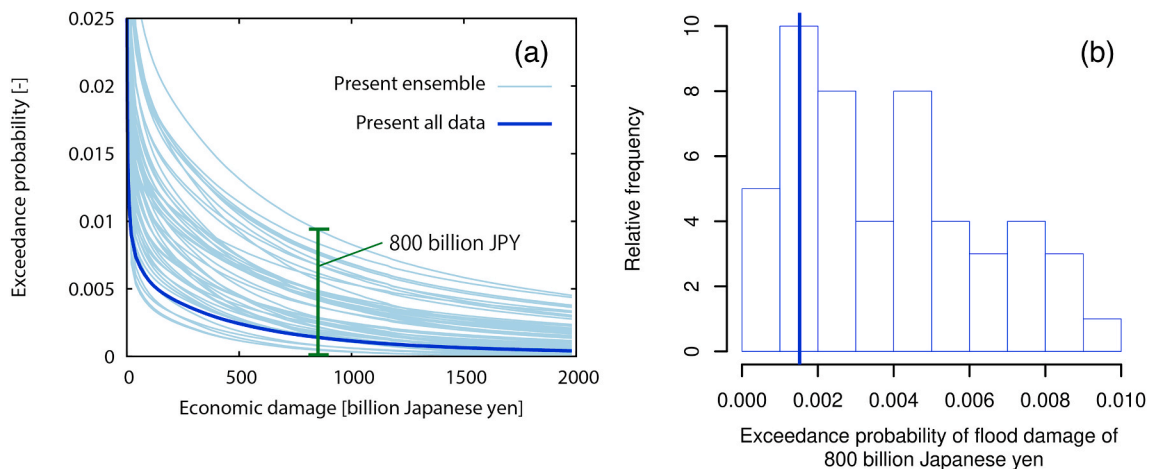


Fig. 10. Estimated flood risk curves in Yodo River basin using the d4PDF historical experiment. Shown are (a) flood risk curves for 50 ensembles with 60-year rainfall data (thin lines) and for the combined 3000-year rainfall data (thick line); and (b) histogram of the exceedance probability of annual flood damage of 800 billion Japanese yen for the flood risk curve derived from the 3000-year rainfall data (adapted from Tanaka et al., 2018).

of design rainfall in d4PDF (based on confidence intervals of annual maximum daily rainfall) by combining probability limit tests with Bayesian inference. Using known frequentist confidence intervals, this study computed Bayesian credible intervals to determine the uncertainty ranges of extreme rainfalls that do not follow typical probability distributions (such as the normal distribution). In contrast, by combining a probabilistic rainfall model with d4PDF, Tanaka et al. (2018) derived physically-based ensemble flood risk curves without assuming any parametric error distribution. As a result, ensemble flood risk curves in the historic and future experiments (see Fig. 8 in Tanaka et al., 2018) indicate a serious increase of flood risk with large variability. This large variability originates from the different SST patterns prescribed for the AGCM simulations and can be physically interpreted as the inter-annual climate variability of the SST patterns and resulting atmospheric circulation patterns, which will significantly impact regional-scale rainfall and hence river discharges and/or flood damages. Some studies have already begun to analyze how variability (in different SST patterns) can affect atmospheric circulation patterns; for example, Ose et al. (2020) used EOF analysis to determine the source of uncertainty in the southerly wind index (which characterizes the East Asian summer monsoon) among CMIP5 ensembles. It will be crucial in future studies to connect changes between atmospheric circulation and simulated flood risk, in order to conduct robust impact assessments of regional climate change flood risk.

5. Coastal hazards

Climate change due to global warming is expected to have major impacts on coastal regions due to sea level rise, TCs and seasonal storms. Understanding how ocean waves and storm surges will change in the future is important for assessing and adapting to the impacts of climate change on coastal, marine and ocean environments, as well as on engineering-related problems (Mori et al., 2016a; Mori and Takemi, 2016). For example, daily changes to waves will influence the coastal environment, through mechanisms such as wave-induced coastal currents, and beach morphology. Likewise, if extreme coastal hazards due to storm surges and storm waves become more frequent or severe in the future, it will be necessary to consider their effects when designing infrastructures (e.g., coastal dikes) with long-term uses of 50 years or more from the present. Since TC activity is a major factor behind climate change impacts in East Asia, it is valuable to assess climate change impacts on natural coastal hazards using climate projections.

5.1. Storm surge

Storm surge can cause devastating damage in low-lying coastal areas found in such regions as the mega deltas in Asia, North Atlantic, North Sea, etc. Projecting future changes in storm surge due to climate change is challenging because of the low occurrence frequencies in any particular area. In addition, storm surge is sensitive to the intensity, track location, and translation speed of TCs and extra-tropical cyclones (ETCs), making it further difficult to assess climate change impacts. Therefore, there are two approaches for assessing the severity of storm surge for coastal research: (1) scenario-based methods using historical or assumed events; and (2) long-term assessment methods using data from historical reanalyses, GCM/RCM projections (e.g., Yasuda et al., 2014), or statistical methods (e.g., Nakajo et al., 2014).

The scenario-based approach for storm surge typically uses a historical event with the highest occurring surge height for the region of interest. Sometimes a historical event from another place will be used if there is no modern recorded data. In the TOUGOU Program, three major bays in Japan have been studied considering climate change using both dynamical storm surge models with an $O(100\text{ m})$ resolution and statistical models: Tokyo, Osaka and Nagoya (Ise Bay). In one such study, Ninomiya et al. (2017) analyzed storm surge from Typhoon Vera (1959) for Ise Bay; they found that the combination of SST and atmospheric

stability of the future climate condition is important for the PGW experiments and that the range of future change depends highly on the assumed or given climate condition. Several related hazard assessments have also been conducted outside of Japan in East Asia. Studies for Korea by Yang et al. (2017, 2018) indicate that there will be a significant increase in storm surge heights along much of the western Korean coast. In fact, Takayabu et al. (2015) have shown that climate change impacts on storm surge are already apparent; based on a set of ensemble climate experiments, analysis of storm surge from Typhoon Haiyan (2013) shows an average 17% increase since pre-industrial times. Incidentally, Jiang et al. (2015; 2019) investigated economic damages based on scenario-based impact assessments; this is important for determining the relation between hazards and exposure, which will be reviewed more fully in the next section.

Long-term assessment methods using data from historical reanalyses, GCM/RCM projections, or statistical methods can give probabilities of potential extremes. A direct way to assess climate change impacts is to use GCM/RCM projection data. However, climate projections typically use time-slices of 20–30 years for both the present and future climate conditions, and the number of TCs in such a short period is not enough to adequately estimate extreme storm surge heights for a particular location. Increasing the projection period is highly desired and as such, the d4PDF dataset (with long-term ensemble projections of historical and future climate conditions) is ideal for assessing climate change impacts on storm surge.

Mori et al. (2019) examined changes to extreme wind speeds and storm surges using d4PDF and found that global future changes of storm surge will be severe within 15–35°N in the Northern Hemisphere, particularly in East Asia. The projected future changes in extreme winds and storm surges for a 100-year return period are shown in Fig. 11. The future changes in extreme wind speeds are caused by shifts in TC tracks and changes in intensity; likewise, future changes in storm surges have a similar tendency due to the changes in extreme wind speed. Future 100-year return values of storm surge increase 20% along the East Asia–eastern and US–western coasts; future 100-year return values of wind speed increase 10% in these same areas due to TCs. A moderate, future increase within 10% is found in storm surge at higher latitudes. While ETCs were not analyzed in detail in the study, it is necessary to analyze how ETCs and related storm surges will change in the near future.

Changes in the extreme storm surges will depend on the length of the return periods. In addition, the 100-year return values for storm surge will generally be less reliable when a small sample size is used (e.g., if historical or 20–50 years of data is used for analysis); however, this is not a problem when using the d4PDF dataset since the extreme storm surge events can be estimated directly without extrapolation. Analyzing future changes of storm surges in Tokyo and Osaka Bays, Mori et al. (2019) found a 0.3–0.45 m increase in storm surge height with a 100-year return period when using a different regional model. This warmer climate tendency changes however if a shorter return period (<10 years) is used, projecting decreased storm surge heights instead.

5.2. Ocean waves

Long-term changes in both daily and extreme waves is important for the fields of coastal, ocean, and environmental engineering. The first future projections of the global wave climate under a global warming scenario using a dynamical wave model (i.e., dynamical global wave climate projection) was conducted by Mori et al. (2010). Following afterwards, several research groups utilized a similar approach (e.g., Hemer et al., 2012) and a series of these studies (on global wave climate projections) were eventually summarized by Hemer et al. (2013), targeting inclusion in IPCC-AR5. While dynamical wave climate projections were discussed in Chapter 13 of the IPCC-AR5 WGI, the number of projections was quite limited and the uncertainty of the projections were generally large at that early stage (e.g., Hemer et al., 2013). Since

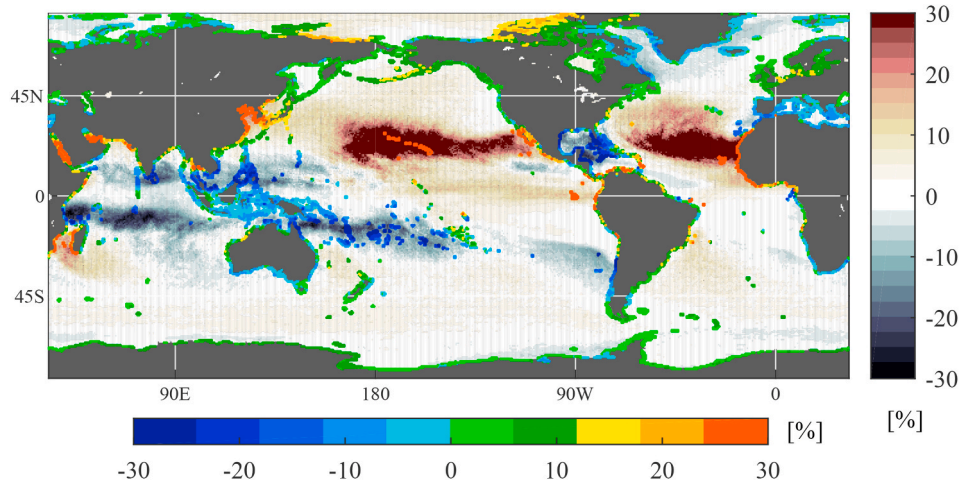


Fig. 11. Future changes [percentage] of 100-year return periods of sea surface wind speed (ocean; right colorbar) and storm surge height (coastline; bottom colorbar) using d4PDF (excerpted from Mori et al., 2019).

the release of IPCC-AR5, efforts to project the future global wave climate have continued by an increasing number of research groups. Phase 2 of the Coordinated Wave Climate Project (COWCLIP2), a world-wide inter-comparison project, coordinated multi-model multi-scenario wave-climate-projections for targeted inclusion in IPCC-AR6. The number of projections has increased greatly since IPCC-AR5 and Morim et al. (2019) has summarized 148 members of global wave climate projections from 21 research groups that participated in COWCLIP2. They identified the future projected changes in the proximity of the world’s coastlines for three annual mean characteristics: wave height, wave period, and wave direction (Fig. 12). Robust changes in wave characteristics are projected over large sectors off of the world’s coasts (covering approximately 50% of the coastline). While there are regions where robust changes are isolated to a single characteristic, there are

large coastal sectors (approximately 40% of the global coastline) where robust changes in wave height, wave period, and/or wave direction coincide. In addition, there are robust, significant changes in future projections of wave direction in the proximity of several coastlines, with magnitudes ranging between $\pm 17^\circ$.

In the WNP region, several wave climate projection studies have been conducted by Shimura et al. (2015a; 2015b; 2016a) using a single-GCM single-wave model ensemble approach. The wave climate projections are based on ensemble climate simulations under the SRES A1B using MRI-AGCM 3.2H (60-km-mesh; Mizuta et al., 2012); time-slice experiments were performed using the periods 1979–2003 and 2075–2099 for the present and future climates (respectively). The wave climate projection consists of 12 ensembles, containing different combinations of (1) varying spatial patterns of future SST and (2)

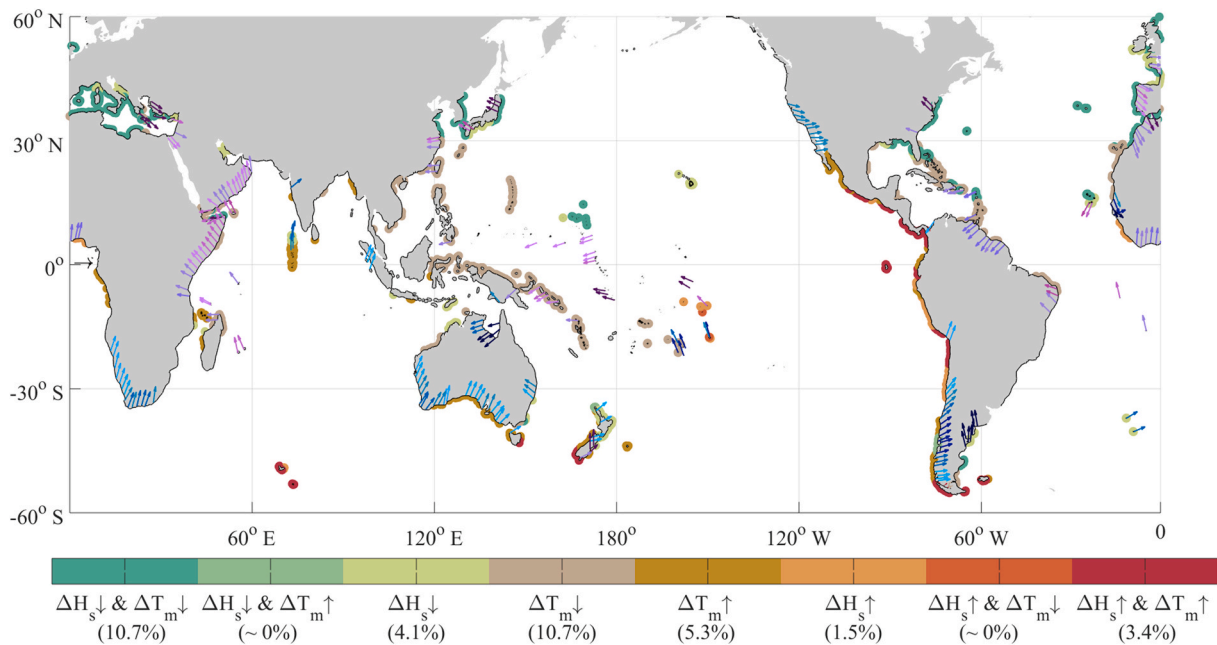


Fig. 12. Projected robust changes in offshore significant wave height ($\overline{H_s}$), period ($\overline{T_m}$) and direction ($\overline{\theta_m}$) by 2080–2100 (under RCP8.5) in the proximity of the world’s coastlines. Sections exhibiting robust weighted multi-member mean changes under RCP8.5 are colored according to the qualitative colorbar (bottom), which also shows the percentage of affected coastline where changes are robust for each wave characteristic(s) (excerpted from Morim et al., 2019).

cumulus convection scheme; the wave climate simulations were generated using the 3rd generation spectral wave model, WAVEWATCH III (Tolman, 2009). Analyzing the wave climate projection, it was found that future changes in the annual mean wave heights in the WNP are projected to range from about ± 0.3 m. Seasonally, future projected changes in summertime mean wave heights, which are influenced by TC changes, vary significantly depending on the spatial SST pattern over the tropical Pacific (Shimura et al., 2015a). In contrast, wintertime wave heights are highly consistent among the ensembles and are projected to decrease overall (Shimura et al., 2016a). In terms of extreme wave heights, future projections of 10-year return-period wave heights generated by TCs, show both increases and decreases from the present climate ranging from ± 4 m for different regions within the WNP (Shimura et al., 2015b).

Discussions of wave climate changes in the IPCC-AR5 and from COW-CLIP2 (e.g., Morim et al., 2019) are mainly based on multi-model ensembles of low-resolution GCMs, with resolutions coarser than 100 km. Shimura et al. (2016b) analyzed projected future changes in extreme wave climate in relation with a GCM's performance in reproducing TC characteristics. Fig. 13 shows the projected future changes in annual maximum wave heights in comparison among the high-resolution MRI-AGCMs and low-resolution GCMs results. Future changes in extreme wave climate

projected by high-resolution MRI-AGCMs show large increases in wave height near Japan and East Asia but large decreases over the south-western part of the WNP. The large decreases in the WNP can be attributed to a decrease in the number of TCs. Future changes projected by all the low-resolution models with high TC performance are spatially inconsistent. Although the projected changes in the TC-generated wave heights show coherent decreases in some models, there is a large variation in the projected changes among the models. On the other hand, future changes projected by all the low-resolution models with low TC performance are mainly dominated by changes in non-TC-generated waves, showing robust decreases in wave heights around latitudes of 30°N. While there is a large variation in the projected changes in the TC-generated waves among all the models, the magnitude of change is 2 times larger than those of non-TC waves. Therefore, an appropriate interpretation of projected TC-generated wave changes and variations (which has been overlooked in previous studies), is important for risk assessment, given the expected larger changes and consequent risks. Timmermans et al. (2017) also described the importance of TC-generated waves in an extreme wave climate projection.

Further applications of wave climate projections are highly expected. One example is of a sandy beach erosion due to climate change. Sea level rise is the most important factor for beach morphology change (e.g. Mori

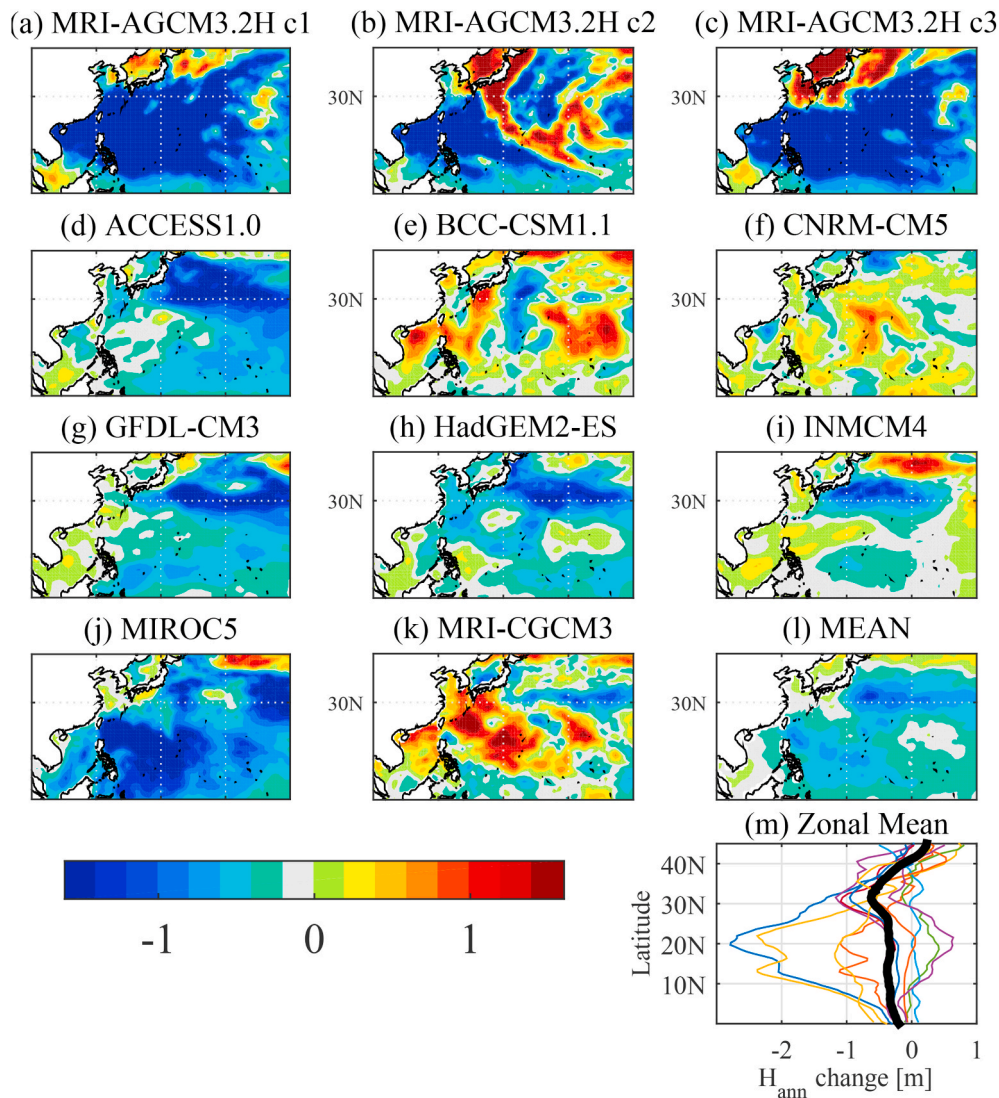


Fig. 13. Projected future changes in mean annual maximum wave heights in the WNP for (a)–(c) MRI-AGCM3.2H under three future SST conditions (c1, c2 and c3) and (d)–(k) eight CMIP5 models with (l) ensemble mean and (m) zonal mean (unit: m). In panel (m), black thick line and colored thin lines are for ensemble mean and each model (respectively). Low-resolution high TC performance models are in panels (e), (f), (j), and (k) (excerpted from Shimura et al., 2016b).

et al., 2018). However, wave climate change can contribute to dynamic changes in beach morphology through onshore/offshore sediment transport (Bennett et al., 2019). The compounded effect of storm surges and waves (in addition to sea level rise) also needs to be taken into consideration for integrated impact assessments of coastal extreme sea levels.

6. Economic impact of storm surge

Flood risk from storm surge will increase because of climate change (Nicholls, 1999; Bengtsson, 2001; Goldenberg et al., 2001; Emanuel, 2005; Hinkel et al., 2014; Muis et al., 2016). Projections of storm surge risk often include uncertainty. Uncertainty can be classified into “risk” (or “aleatory uncertainty”) and “ambiguity” (also called “epistemic uncertainty” or “deep uncertainty”) in economics. The risk refers to the natural randomness of the relevant event and is often represented as by a single well-defined probability distribution function (PDF). The ambiguity refers to situations where there is too little information to specify a single PDF and is often represented by multiple PDFs (Merz and Thieken, 2009; Kunreuther et al., 2013). Ambiguity may stem from insufficient knowledge on parameters and structures of models (model uncertainty) and/or socio-economic situations (socio-economic scenario uncertainty) (Camerer and Weber, 1992; Etner et al., 2012). Storm surge risks include ambiguity caused from an insufficient knowledge of TC systems, such as cyclogenesis factors, developmental processes, and movement (Henderson-Sellers et al., 1998; Knutson et al., 2010; Grinstead, 2013; Little, 2015; Wong and Keller, 2017). Thus, policy makers should design and implement adaptation policies with ambiguity or based on multiple projections of storm surge risk.

6.1. Economic evaluation of storm surge risk mitigation policy under ambiguity

Generally, an engineering-based adaptation design (e.g., raising an embankment) needs deterministic design values for a particular return period and event (e.g., height of extreme sea level). However, design values will change over time because of climate change and the uncertainty of changes (in these values) needs to be considered. Therefore, a flexible adaptation strategy is needed in comparison with present design procedures.

Previously, extensive studies have estimated the economic value of possessing a policy mitigating storm surge flood risk (Botzen et al., 2009; Botzen and van den Bergh, 2012; Withey et al., 2019). However, these studies ignored ambiguity when projecting the storm surge risks. Several studies have also explored the ambiguity of storm surge risks (Hallegatte et al., 2011; Resio et al., 2013; Wong and Keller, 2017; Oddo et al., 2017) and proposed decision support methods under ambiguity (Hunter, 2012; Buchanan et al., 2016; Srivier et al., 2018; Rohmer et al., 2019). However, these studies did not consider a general public preference on ambiguity. Since many studies have found that general public decisions are often affected by ambiguity (Camerer and Weber, 1992; Etner et al., 2012), decisions by policy makers should reflect the general public's preferences on ambiguity.

As such, Theme D of the TOUGOU Program has been conducting novel economic impact studies that evaluate the economic value of adaptation policies which mitigate storm surge risk under ambiguity (Fujimi et al., 2021). In one study, Fujimi et al. (2021) estimated general public preferences on risk and ambiguity of storm surge risk and evaluated the economic value of a mitigation policy for reducing storms surges based on the estimated preferences. This study will be reviewed in depth as a case study in the next subsection.

6.2. Case study: Osaka Bay in Japan

Fujimi et al. (2021) estimated the economic values of a dike rising policy under ambiguity, to mitigate storm surge risk in Osaka Bay, Japan

(Fig. 14). Over 200 years of TC simulations in Osaka Bay were generated using the Global Stochastic Tropical Cyclone Model (Nakajo et al., 2014), with an assumed increased TC intensity based on the maximum potential intensity (MPI) from CMIP5 experiments (Ariyoshi and Mori, 2018). The four worst-case simulated TCs were then selected among the 200-year period. Their properties (e.g., track, speed, central pressure) were used in a fully-coupled surge-wave-tide model (SUWAT; Kim et al., 2008) to predict the resulting storm surges, and then calculate the 30-m-mesh flood depths in Osaka Bay with a model developed by Liang et al. (2010). The above process produced a single PDF of storm surge flood risk in each cell for over a 200-year period. To explore ambiguity, this process was repeated 25 times to obtain 25 PDFs of storm surge flood risk.

Fujimi et al. (2021) then implemented a web-based survey for ordinary people living in the Osaka Bay area. In this survey, respondents were asked to state their willingness to pay for eliminating storm surge risk and ambiguity through choice experiments on the purchase of a hypothetical full coverage insurance after be presented with the predicted storm surge risk and ambiguity in their area of residence. Using the survey data, their preferences on risk and ambiguity were estimated using a Limited Degree of Confidence (LDC) model. Many decision models have been proposed for dealing with ambiguity (Ryan, 2009; Etner et al., 2012; Lempert et al., 2006; Machina and Siniscalchi 2014; Gilboa and Marinacci 2016) and the LDC model has often been applied in the context of climate change (Lange, 2003; Froyen, 2005; McInerney et al., 2012; Buchannan et al., 2016). This model is a specification of a neo-additive model developed by Chateauneuf et al. (2007), which is a generalized form of the Choquet expected utility model (Schmeidler 1989) and the α -maximin expected utility model (Ghirardato et al., 2004).

In the web-survey choice experiment, an individual following the LDC model focuses on the average and worst PDFs under ambiguity as represented by the 25 PDFs of storm surge flood risk. He or she makes a decision by weighing the PDF with an ambiguity attitude parameter ranging from zero to one. The estimated preferences from the LDC model indicate that the sample average of the ambiguity attitude parameter was around 0.1, indicating that the sample average respondent made a decision by weighing the worst PDF with 10% and the average PDF with 90%. That is, the worst PDF was overemphasized due to the ambiguity attitude since the worst PDF must be weighted in proportion to the number of PDFs (1/25) when ignoring the ambiguity attitude.

The economic value of a policy mitigating storm surge risk by rising a dike by 1 m, was calculated using the estimated LDC model. For investigating the ambiguity effect, the economic value was decomposed into three parts: expected loss reduction, risk premium, and ambiguity premium. The risk premium is the economic value caused from eliminating risk, or natural randomness of the storm surge event. The ambiguity premium is the economic value for eliminating ambiguity, or specifying a single PDF from multiple PDFs of storm surge risk.

The geographical distributions of the expected loss reductions, risk premiums, and uncertainty premiums for a dike rise by 1 m are illustrated in Fig. 15 for current and future (i.e., 10 hPa reduction in TC center and sea level rise by 0.85 m) climate conditions. These figures indicate that the risk and uncertainty premiums are not negligible in size and occur unevenly among areas where there is risk of flood damage. These results suggest that risk and uncertainty premiums cannot be ignored when evaluating the economic value of a policy that mitigates storm surge flood risk under ambiguity.

7. Conclusions

This manuscript has reviewed research activity of the TOUGOU Program on natural hazards. The latest results indicate an increase in TC- and Baiu-related natural hazards due to climate change in Japan and East Asia. Fig. 16 shows a graphical summary of the major research results, and the findings are summarized below.

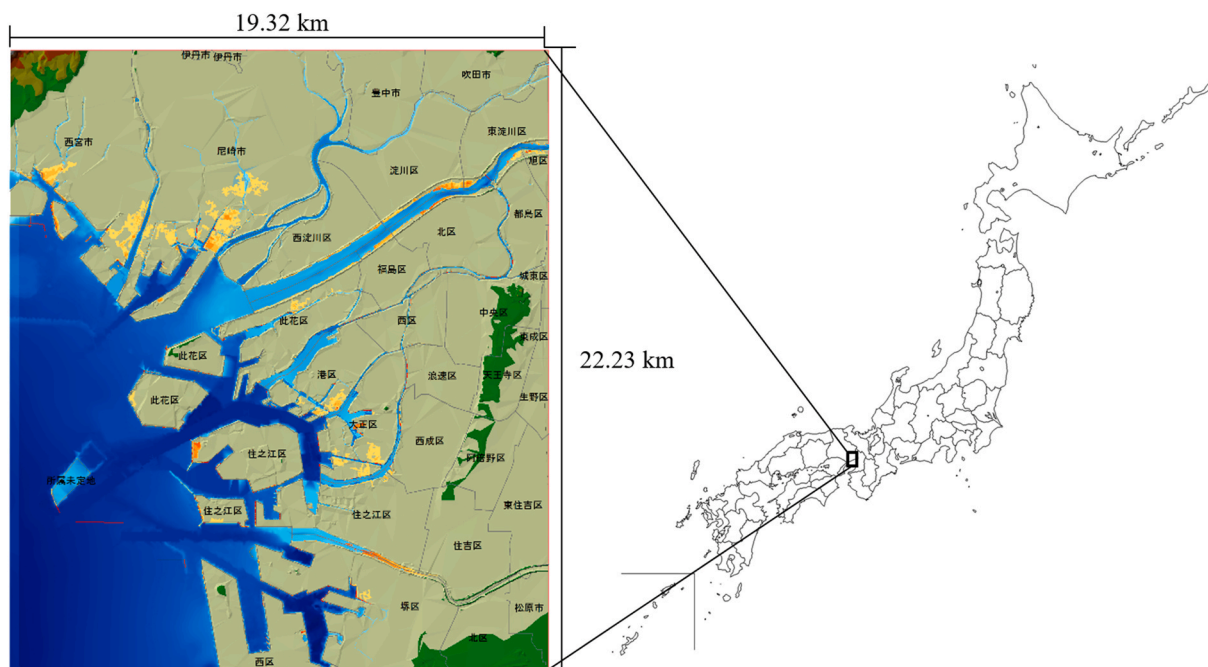


Fig. 14. Research area in Osaka Bay (appears in Fujimi et al., 2021).

The PGW experiment is a technique to downscale particular events considering incremental climate change and is a powerful method to estimate future changes in TC characteristics and related hazards. As a common response to TCs in a warmer climate condition, analyses for Typhoon Vera and Talas indicate that rainfall and wind hazards on the Pacific side of Japan are projected to be harsher under the PGW condition. Wind intensity will also be stronger under the PGW condition. In contrast, TC impacts in northern Japan are mixed and differ from those on the southern-facing Pacific side of Japan. Analyses of Typhoons Songda and Mireille indicate wind hazards over Hokkaido and northern Japan will become less severe under the PGW condition; however, analyses of Typhoons Chanthu, Lionrock, and others indicate that the amount of TC-induced rainfall in northern Japan is projected to increase under the warmer climate condition. A larger amount of convective available potential energy in the PGW condition is shown to contribute to stronger updrafts and hence increased rainfall in the TC core regions.

Besides TC-related precipitation, future changes of Baiu precipitation are strongly controlled by particular, atmospheric circulation features within a model. The occurrence frequency of Baiu localized extreme rainfall is projected to increase in future climate conditions and an increasing trend has been identified in the accumulated amount of extreme rainfall. The rate of increase in rainfall intensity was examined further through comparisons with a CC relationship and it was found that the rate of increase for extreme rainfall intensity is $\sim 3\% \text{ } ^\circ\text{C}^{-1}$ in the present climate and is anticipated to rise to $\sim 3.5\% \text{ } ^\circ\text{C}^{-1}$ under future climate conditions. In addition, projections of Guerrilla-heavy rainfall, or rapidly developing isolated thunderstorms, were analyzed using an RCM. The future change of the smaller scale Guerrilla-heavy rainfall shows an increasing trend in the occurrence frequency for August around the Kansai region in Japan. Total atmospheric destabilization was identified as the possible cause for the increased Guerrilla-heavy rainfall.

A projection of extreme river flooding using d4PDF found that future river discharges will change in highly-urbanized basins of Japan. Future changes in the probability distributions of extreme rainfall events and magnitudes of the largest class of floods state that the 200-year annual

maximum 24-h rainfall for the d4PDF future experiment is 1.3–1.4 times larger than the historic experiment, and likewise, the annual maximum river discharge is 1.5–1.7 times larger over Japan, generally. As a result, ensemble flood risk curves in the historic and future experiments indicate a serious increase of flood risk with large variability.

Future changes in storm surges and waves were examined using scenario-based (surge only) and long-term assessment methods based on GCM projections or statistical methods, depending on the spatial and temporal resolutions needed. Severe storm surges and extreme waves will be less frequent but more intense in the realized future climate conditions. In regional analyses using the d4PDF dataset, storm surge heights with a 100-year return period in Tokyo and Osaka Bays are projected to increase by 0.3–0.45 m. Furthermore, extreme waves by TCs are projected to decrease in the south-western part of the WNP but increase near Japan and East Asia. While there is large variation in the future changes of TC-generated waves among an ensemble of GCM projections, the magnitude of change is 2 times larger than those of non-TC waves and warrants focus for risk assessment.

General public decisions are often affected by ambiguity, so it is important to consider mitigation costs in addition to adaptation costs when developing an adaptation strategy. Accordingly, a summary was presented on (1) estimating the general public preferences on risk and ambiguity of storm surge risk and (2) evaluating the economic value of a mitigation policy for reducing storms surges based on the estimated preferences. The economic value of a dike rising policy under ambiguity was then estimated to mitigate storm surge risk in Osaka Bay, Japan. Risk and uncertainty premiums cannot be ignored when evaluating the economic value of a policy that mitigates storm surge flood risk under ambiguity.

The impacts of climate change on many TC- or Baiu-related natural hazards in Japan and East Asia have been reviewed here. We have used both scenario-based (GHGE) GCM climate projections (mainly d4PDF here) and PGW experiments for assessing climate hazards. While climate projections are straight-forward to create and generate consistent climatologies, they have limited spatial resolutions and temporal lengths. In addition, even though challenges related to temporal length can be

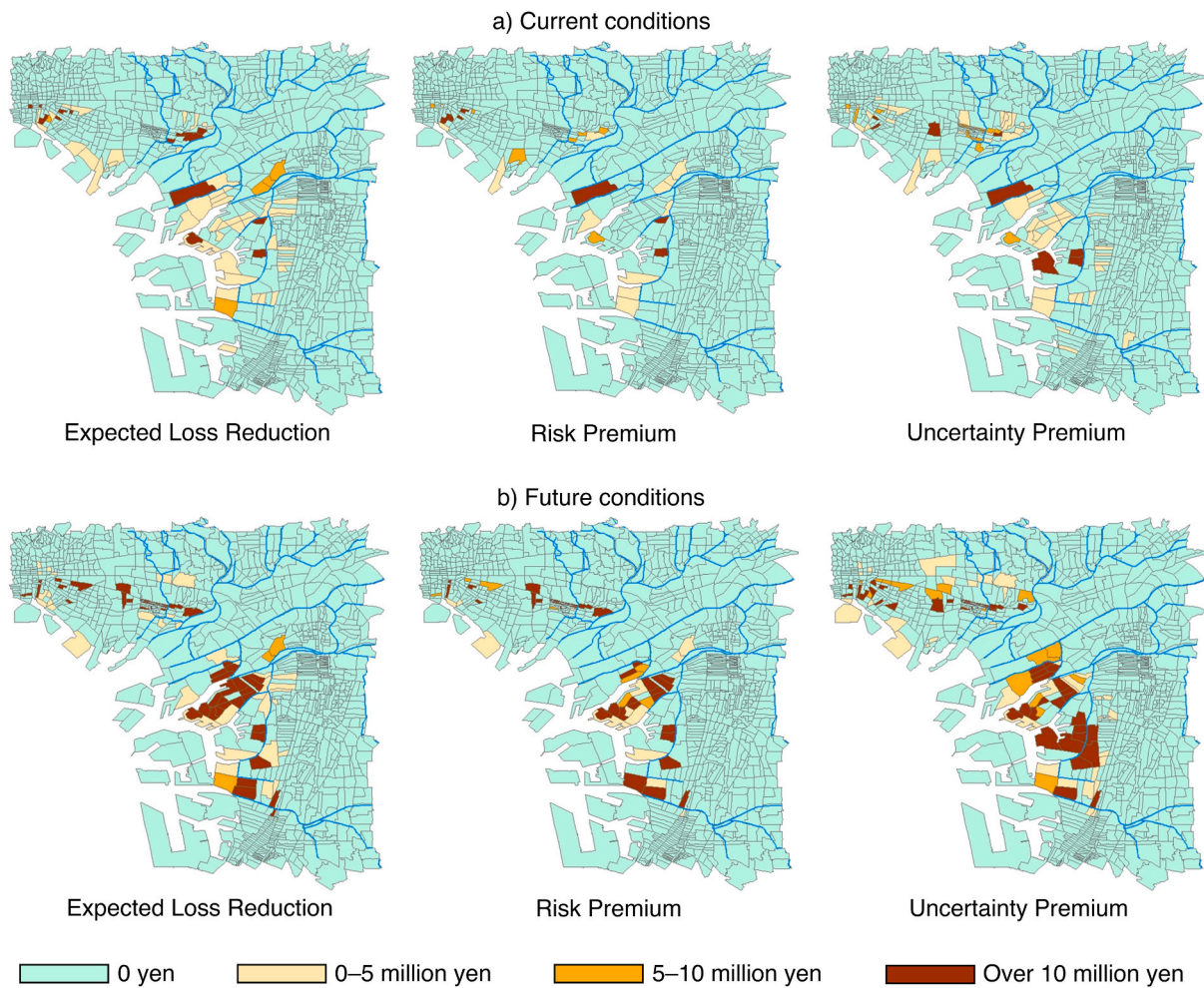


Fig. 15. Case study in Osaka Bay, Japan. Shown are expected loss reductions, risk premiums, and uncertainty premiums for a 1 m dike rise mitigation policy for (a) current and (b) future conditions (appears in Fujimi et al., 2021).

overcome using the d4PDF dataset, spatial resolutions are still coarse globally and bias corrections are necessary for real-world applications. On the other hand, PGW experiments can handle high resolutions up to $O(100\text{ m})$ and are a powerful method for assessing how historically important events might change under future climate conditions. However, it is difficult to estimate probability information accurately from a PGW experiment since the number of available events depends on previously occurred events. Therefore, a combination of the two approaches are important for conducting impact assessment of extreme events.

While the assessments showed significant changes in the future, it is important to know the probabilistic risk of a hazard with uncertainty due to climate change. As shown in Fig. 1, correcting bias in a climate projection is an essential issue for adaptation planning (e.g., technical and social implementation); it will be crucial for future research to utilize observations and develop standard methods for correcting biases in means and extremes. In addition to uncertainty, the interaction of different natural hazards can lead to compound events and it is important to assess their future combined impacts. These are the next steps in assessing climate change impacts for adaptation.

Availability of data and material

Data supporting the conclusions of this article are available upon request. Please contact the authors for further details.

Funding

This work was supported by the Integrated Research Program for Advancing Climate Models (TOUGOU Program) under grant number JPMXD0717935498 (FY2017–FY2021), which is funded by the Ministry of Education, Culture, Sports, Science, and Technology (MEXT), Japan.

Authors’ contributions

TTk contributed to the section on Tropical cyclones. EN, YO, and TTk contributed to the section on Baiu and precipitation. YT and TTn contributed to the section on River flood risk. NM and TS contributed to the section on Coastal Hazards. HT and TF contributed to the section on Economic Impact. NM and AW contributed to the opening and closing sections and compiled the manuscript. All authors read and approved the final manuscript.

Authors’ information

All authors have participated respectively in Theme D: Integrated Hazard Prediction of the Integrated Research Program for Advancing Climate Models (TOUGOU Program).

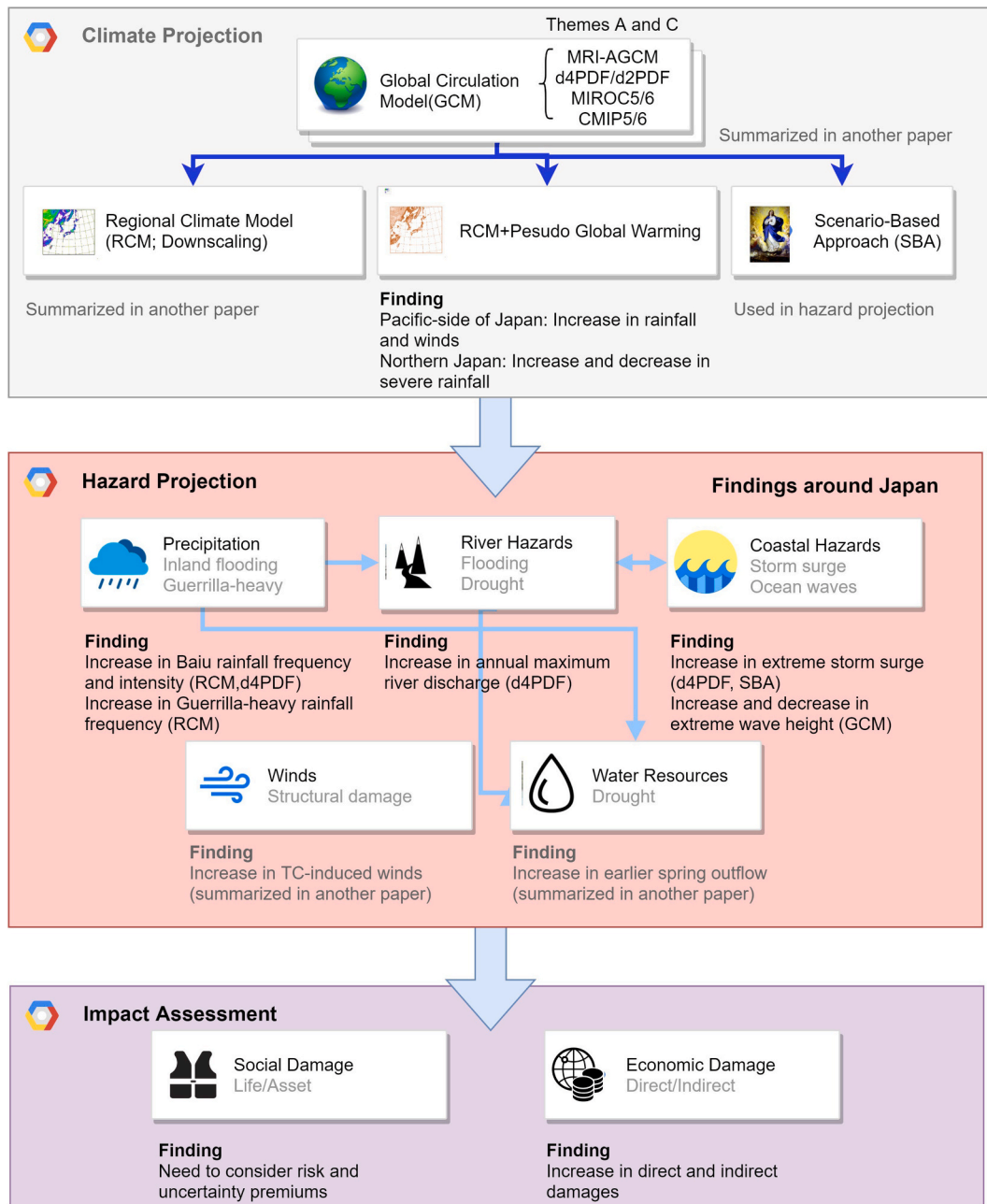


Fig. 16. Summary of research results in this study.

Declaration of competing interest

The authors declare that they have no known competing financial interests or personal relationships that could have appeared to influence the work reported in this paper.

Acknowledgements

This work was supported and conducted by members of the Integrated Research Program for Advancing Climate Models (TOUGOU Program). The authors would like to express gratitude to all members of the group whose contributions were reviewed in this manuscript. The authors also appreciate two anonymous reviewers who provided valuable comments that helped improve the quality of the manuscript.

References

Aalbers, E.E., Lenderink, G., van Meijgaard, E., van den Hurk, B.J.J.M., 2018. Local-scale changes in mean and heavy precipitation in Western Europe, climate change or internal variability? *Clim. Dynam.* 50, 4745–4766. <https://doi.org/10.1007/s00382-017-3901-9>.

Ariyoshi, N., Mori, N., 2018. Future projection of storm surge height at three major bays in Japan using maximum potential intensity of typhoon in western North Pacific. *J. Jpn. Soc. Civ. Eng. Ser. B2 Coast. Eng.* 74 (2), 1_619–1_624 (in Japanese). <https://doi.org/10.2208/kaigan.74.1.619>.

Arnell, N.W., Gosling, S.N., 2016. The impacts of climate change on river flood risk at the global scale. *Climatic Change* 134, 387–401. <https://doi.org/10.1007/s10584-014-1084-5>.

Bengtsson, L., 2001. Hurricane threats. *Science* 293, 440–441. <https://doi.org/10.1126/science.1062047>.

Bennett, W., Karunarathna, H., Reeve, D., Mori, N., 2019. Computational modelling of morphodynamic response of a macro-tidal beach to future climate variabilities. *Mar. Geol.* 415, 105960. <https://doi.org/10.1016/j.margeo.2019.105960>.

Botzen, W.J., Aerts, J.C., van den Bergh, J.C., 2009. Willingness of homeowners to mitigate climate risk through insurance. *Ecol. Econ.* 68 (8), 2265–2277. <https://doi.org/10.1016/j.ecolecon.2009.02.019>.

- Botzen, W.J.W., van den Bergh, J.C.J.M., 2012. Monetary valuation of insurance against flood risk under climate change. *Int. Econ. Rev.* 53 (3), 1005–1025. <https://doi.org/10.1111/j.1468-2354.2012.00709.x>.
- Bryan, G.H., Rotunno, R., 2009. The influence of near-surface, high-entropy air in hurricane eyes on maximum hurricane intensity. *J. Atmos. Sci.* 66, 148–158. <https://doi.org/10.1175/2008JAS2707.1>.
- Buchanan, M.K., Kopp, R.E., Oppenheimer, M., Tebaldi, C., 2016. Allowances for evolving coastal flood risk under uncertain local sea-level rise. *Climatic Change* 137 (3–4), 347–362. <https://doi.org/10.1007/s10584-016-1664-7>.
- Camerer, C., Weber, M., 1992. Recent developments in modeling preferences: Uncertainty and ambiguity. *J. Risk Uncertain.* 5, 325–370. <https://doi.org/10.1007/BF00122575>.
- Chateauneuf, A., Eichberger, J., Grant, S., 2007. Choice under uncertainty with the best and worst in mind: Neo-additive capacities. *J. Econ. Theor.* 137 (1), 538–567. <https://doi.org/10.1016/j.jet.2007.01.017>.
- CSIRO and Bureau of Meteorology, 2015. *Climate Change in Australia, Information for Australia's Natural Resource Management Regions: Technical Report*. CSIRO and Bureau of Meteorology, Australia, p. 216.
- CSIRO and Bureau of Meteorology, 2020. *Climate Change in Australia*. <https://www.climatechangeinaustralia.gov.au>. (Accessed 3 June 2020).
- Emanuel, K.A., 1986. An air-sea interaction theory for tropical cyclones. Part I: Steady-state maintenance. *J. Atmos. Sci.* 43, 585–605. [https://doi.org/10.1175/1520-0469\(1986\)043<0585:AASITF>2.0.CO;2](https://doi.org/10.1175/1520-0469(1986)043<0585:AASITF>2.0.CO;2).
- Emanuel, K., 2005. Increasing destructiveness of tropical cyclones over the past 30 years. *Nature* 436, 686–688. <https://doi.org/10.1038/nature03906>.
- Etner, J., Jeleva, M., Tallon, J.M., 2012. Decision theory under ambiguity. *J. Econ. Surv.* 26, 234–270. <https://doi.org/10.1111/j.1467-6419.2010.00641>.
- Fischer, E., Knutti, R., 2016. Observed heavy precipitation increase confirms theory and early models. *Nat. Clim. Change* 6, 986–991. <https://doi.org/10.1038/nclimate3110>.
- Froyen, C.B., 2005. Decision criteria, scientific uncertainty, and the global warming controversy. *Mitig. Adapt. Strategies Glob. Change* 10 (2), 183–211. <https://doi.org/10.1007/s11027-005-3782-9>.
- Fujimi, T., Jiang, X., Mori, N., Tatano, H., Nakakita, E., Watanabe, M., Begum, R.A., 2021. Preferences of storm surge risk mitigation under ambiguity: The case of Osaka Bay in Japan. In preparation.
- Ghirardato, P., Maccheroni, F., Marinacci, M., 2004. Differentiating ambiguity and ambiguity attitude. *J. Econ. Theor.* 118 (2), 133–173. <https://doi.org/10.1016/j.jet.2003.12.004>.
- Gilboa, I., Marinacci, M., 2016. *Ambiguity and the Bayesian paradigm*. In: *Readings in Formal Epistemology*. Springer, Cham, pp. 385–439.
- Goldenberg, S.B., Landsea, C.W., Mestas-Nunez, A.M., Gray, W.M., 2001. The recent increase in Atlantic hurricane activity: Causes and implications. *Science* 293, 474–479. <https://doi.org/10.1126/science.1060040>.
- Grinstead, A., Moore, J.C., Jevrejeva, S., 2013. Projected Atlantic hurricane surge threat from rising temperatures. *Proc. Natl. Acad. Sci. U. S. A* 110 (14), 5369–5373. <https://doi.org/10.1073/pnas.1209980110>.
- Gutmann, E.D., Rasmussen, R.M., Liu, C., Ikeda, K., Bruyere, C.L., Done, J.M., Garré, L., Friis-Hansen, P., Veldore, V., 2018. Changes in hurricanes from a 13-yr convection-permitting pseudo-global warming simulation. *J. Clim.* 31 (9), 3643–3657. <https://doi.org/10.1175/JCLI-D-17-0391.1>.
- Hagos, S.M., Leung, L.R., Yoon, J.-H., Lu, J., Gao, Y., 2016. A projection of changes in landfalling atmospheric river frequency and extreme precipitation over western North America from the Large Ensemble CISM simulations. *Geophys. Res. Lett.* 43, 1357–1363. <https://doi.org/10.1002/2015GL067392>.
- Hallegratte, S., Ranger, N., Mestre, O., Dumas, P., Corfee-Morlot, J., Herweijer, C., Wood, R.M., 2011. Assessing climate change impacts, sea level rise and storm surge risk in port cities: A case study on Copenhagen. *Climatic Change* 104 (1), 113–137. <https://doi.org/10.1007/s10584-010-9978-3>.
- Harada, M., Maruya, Y., Kojima, T., Matsuoka, D., Nakagawa, Y., Kawahara, S., Arai, F., 2018. Flood frequency analysis and impact assessment for climate change in the Nagara River basin. *J. Jpn. Soc. Civ. Eng. Ser. B1 Hydraul. Eng.* 74 (4), 1181–1186 (in Japanese). <https://doi.org/10.2208/jsejhe.74.1181>.
- Hatsuzuka, D., Sato, T., 2019. Future changes in monthly extreme precipitation in Japan using large-ensemble regional climate simulations. *J. Hydrometeorol.* 20 (3), 563–574. <https://doi.org/10.1175/JHM-D-18-0095.1>.
- Hemer, M.A., Fan, Y., Mori, N., Semedo, A., Wang, X.L., 2013. Projected changes in wave climate from a multi-model ensemble. *Nat. Clim. Change* 3, 471–477. <https://doi.org/10.1038/nclimate1791>.
- Hemer, M.A., Katzfey, J., Trenham, C., 2012. Global dynamical projections of surface ocean wave climate for a future high greenhouse gas emission scenario. *Ocean Model.* 70, 221–245. <https://doi.org/10.1016/j.ocemod.2012.09.008>.
- Henderson-Sellers, A., Zhang, H., Berz, G., Emanuel, K., Gray, W., Landsea, C., Holland, G., Lighthill, J., Shieh, S.-L., Webster, P., McGuffie, K., 1998. Tropical cyclones and global climate change: A post-IPCC assessment. *Bull. Am. Meteorol. Soc.* 79, 19–38. [https://doi.org/10.1175/1520-0477\(1998\)079<0019:TCAGCC>2.0.CO;2](https://doi.org/10.1175/1520-0477(1998)079<0019:TCAGCC>2.0.CO;2).
- Hersbach, H., Bell, B., Berrisford, P., Hirahara, S., Horányi, A., Muñoz-Sabater, J., Nicolas, J., Peubey, C., Radu, R., Schepers, D., Simmons, A., Soci, C., Abdalla, S., Abellan, X., Balsamo, G., Bechtold, P., Biavati, G., Bidlot, J., Bonavita, M., De Chiara, G., Dahlgren, P., Dee, D., Diamantakis, M., Dragani, R., Flemming, J., Forbes, R., Fuentes, M., Geer, A., Haimberger, L., Healy, S., Hogan, R.J., Hólm, E., Janisková, M., Keeley, S., Lalouaux, P., Lopez, P., Lupu, C., Radnoti, G., de Rosnay, P., Rozum, I., Vamborg, F., Villaume, S., Thépaut, J.N., 2020. The ERA5 global reanalysis. *Q. J. R. Meteorol. Soc.* 146, 1999–2049. <https://doi.org/10.1002/qj.3803>.
- Hill, K.A., Lackmann, G.M., 2011. The impact of future climate change on TC intensity and structure: A downscaling approach. *J. Clim.* 24, 4644–4661. <https://doi.org/10.1175/2011JCLI3761.1>.
- Hinkel, J., Lincke, D., Vafeidis, A.T., Perrette, M., Nicholls, R.J., Tol, R.S.J., Marzeion, B., Fettweis, X., Ionescu, C., Levermann, A., 2014. Coastal flood damage and adaptation costs under 21st century sea-level rise. *Proc. Natl. Acad. Sci. U.S.A.* 111 (9), 3292–3297. <https://doi.org/10.1073/pnas.1222469111>.
- Hirabayashi, Y., Mahendran, R., Koirala, S., Konoshima, L., Yamazaki, D., Watanabe, S., Kim, H., Kanae, S., 2013. Global flood risk under climate change. *Nat. Clim. Change* 3 (9), 816–821. <https://doi.org/10.1038/nclimate1911>.
- Hirahara, S., Ohno, H., Oikawa, Y., Maeda, S., 2012. Strengthening of the southern side of the jet stream and delayed withdrawal of Baiu season in future climate. *J. Meteorol. Soc. Jpn. Ser. II* 90, 663–671. <https://doi.org/10.2151/jmsj.2012-506>.
- Hirokawa, Y., Kato, T., Tsuguti, H., Seino, N., 2020. Identification and classification of heavy rainfall areas and their characteristic features in Japan. *J. Meteorol. Soc. Jpn. Ser. II* 98 (4), 835–857. <https://doi.org/10.2151/jmsj.2020-043>.
- Hoshino, T., Yamada, T., 2018. Analysis of annual maximum precipitation over first-class river domains in Japan using a large-ensemble dataset (d4PDF). *J. Jpn. Soc. Civ. Eng. Ser. B1 Hydraul. Eng.* 74 (4), 1187–1192 (in Japanese). <https://doi.org/10.2208/jsejhe.74.1187>.
- Hsu, H.H., Chou, C., Wu, Y.C., Lu, M.M., Chen, C.T., Chen, Y.M., 2011. *Climate Change in Taiwan: Scientific Report 2011 (Summary)*. National Science Council, Taipei, Taiwan, ROC, p. 67.
- Hunter, J., 2012. A simple technique for estimating an allowance for uncertain sea-level rise. *Climatic Change* 113, 239–252. <https://doi.org/10.1007/s10584-011-0332-1>.
- IPCC (2013) *Climate Change 2013: The Physical Science Basis*. Contribution of Working Group I to the Fifth Assessment Report of the Intergovernmental Panel on Climate Change. [Stocker TF, Qin D, Plattner G-K, Tignor M, Allen SK, Boschung J, Nauels A, Xia Y, Bex V, Midgley PM (eds)]. Cambridge University Press, Cambridge, United Kingdom and New York, NY, USA, 1535 pp. <https://doi.org/10.1017/CBO9781107415324>.
- IPCC (2014) *Climate Change 2014: Impacts, Adaptation, and Vulnerability*. Part B: Regional Aspects. Contribution of Working Group II to the Fifth Assessment Report of the Intergovernmental Panel on Climate Change [Barros VR, Field CB, Dokken DJ, Mastrandrea MD, Mach KJ, Bilir TE, Chatterjee M, Ebi KL, Estrada YO, Genova RC, Girma B, Kissel ES, Levy AN, MacCracken S, Mastrandrea PR, White LL (eds)]. Cambridge University Press, Cambridge, United Kingdom and New York, NY, USA, 688 pp.
- IPCC, 2019. *IPCC Special Report on the Ocean and Cryosphere in a Changing Climate* [Pörtner, H.-O., Roberts, D.C., Masson-Delmotte, V., Zhai, P., Tignor, M., Poloczanska, E., Mintenbeck, K., Nicolai, M., Okem, A., Petzold, J., Rama, B., Weyer, N. (eds.)]. In press.
- Ishii, M., Mori, N., 2020. d4PDF: Large-ensemble and high-resolution climate simulations for global warming countermeasures. *Prog. Earth Planet. Sci.* 7 (58) <https://doi.org/10.1186/s40645-020-00367-7>.
- Ishikawa, H., Oku, Y., Kim, S., Takemi, T., Yoshino, J., 2013. Estimation of a possible maximum flood event in the Tone River basin, Japan caused by a tropical cyclone. *Hydro. Process.* 27, 3292–3300. <https://doi.org/10.1002/hyp.9830>.
- Ito, R., Takemi, T., Arakawa, O., 2016. A possible reduction in the severity of typhoon wind in the northern part of Japan under global warming: A case study. *SOLA* 12, 100–105. <https://doi.org/10.2151/sola.2016-023>.
- Jiang, X., Mori, N., Tatano, H., Yang, L., Shibutani, Y., 2015. Estimation of property loss and business interruption loss caused by storm surge inundation due to climate change: A case of Typhoon Vera revisited. *Nat. Hazards* 84, 35–49. <https://doi.org/10.1007/s11069-015-2085-z>.
- Jiang, X., Mori, N., Tatano, H., Yang, L., 2019. Simulation-based exceedance probability curves to assess economic impacts of storm surge inundation under climate change scenarios: A case study in Ise Bay, Japan. *Sustainability* 11 (4), 1090. <https://doi.org/10.3390/su11041090>.
- Kanada, S., Tsuboki, K., Takayabu, I., 2020. Future changes of tropical cyclones in the midlatitudes in 4-km-mesh downscaling experiments from large-ensemble simulations. *SOLA* 16, 57–63. <https://doi.org/10.2151/sola.2020-010>.
- Kanada, S., Aiki, H., Tsuboki, K., Takayabu, I., 2019. Future changes in typhoon-related precipitation in eastern Hokkaido. *SOLA* 15, 244–249. <https://doi.org/10.2151/sola.2019-044>.
- Kanada, S., Nakano, M., Kato, T., 2012. Projections of future changes in precipitation and the vertical structure of the frontal zone during the Baiu season in the vicinity of Japan using a 5-km-mesh regional climate model. *J. Meteorol. Soc. Jpn. Ser. II* 90A, 65–86. <https://doi.org/10.2151/jmsj.2012-A03>.
- Kanada, S., Takemi, T., Kato, M., Yamasaki, S., Fudeyasu, H., Tsuboki, K., Arakawa, O., Takayabu, I., 2017a. A multi-model intercomparison of an intense typhoon in future, warmer climates by four 5-km-mesh models. *J. Clim.* 30, 6017–6036. <https://doi.org/10.1175/JCLI-D-16-0715.1>.
- Kanada, S., Tsuboki, K., Aiki, H., Tsujino, S., Takayabu, I., 2017b. Future enhancement of heavy rainfall events associated with a typhoon in the midlatitude regions. *SOLA* 13, 246–251. <https://doi.org/10.2151/sola.2017-045>.
- Kato, T., 2020. Quasi-stationary band-shaped precipitation systems, named “senjokousuitai”, causing localized heavy rainfall in Japan. *J. Meteorol. Soc. Jpn. Ser. II* 98, 485–509. <https://doi.org/10.2151/jmsj.2020-029>.
- Kawabata, T., Kuroda, T., Seko, H., Saito, K., 2011. A cloud-resolving 4DVAR assimilation experiment for a local heavy rainfall event in the Tokyo metropolitan area. *Mon. Weather Rev.* 139 (6), 1911–1931. <https://doi.org/10.1175/2011MWR3428.1>.
- Kawase, H., Yoshikane, T., Hara, M., Kimura, F., Yasunari, T., Ailikon, B., Ueda, H., Inoue, T., 2009. Intermodel variability of future changes in the Baiu rainband

- estimated by the pseudo global warming downscaling method. *J. Geophys. Res.* 114, D24110. <https://doi.org/10.1029/2009JD011803>.
- Kay, J.E., Deser, C., Phillips, A., Mai, A., Hannay, C., Strand, G., Arblaster, J.M., Bates, S.C., Danabasoglu, G., Edwards, J., Holland, M., Kushner, P., Lamarque, J.F., Lawrence, D., Lindsay, K., Middleton, A., Munoz, E., Neale, R., Oleson, K., Polvani, L., Vertenstein, M., 2015. The Community Earth System Model (CESM) Large Ensemble project: A community resource for studying climate change in the presence of internal climate variability. *Bull. Am. Meteorol. Soc.* 96 (8), 1333–1349. <https://doi.org/10.1175/BAMS-D-13-00255.1>.
- Kida, H., Koide, T., Sasaki, H., Chiba, M., 1991. A new approach for coupling a limited area model to a GCM for regional climate simulations. *J. Meteorol. Soc. Jpn.* 69, 723–728. <https://doi.org/10.2151/jmsj1965.69.6.723>.
- Kim, S.Y., Yasuda, T., Mase, H., 2008. Numerical analysis of effects of tidal variations on storm surges and waves. *Appl. Ocean Res.* 30 (4), 311–322. <https://doi.org/10.1016/j.apor.2009.02.003>.
- Kitoh, A., Uchiyama, T., 2006. Changes in onset and withdrawal of the East Asian summer rainy season by multi-model global warming experiments. *J. Meteorol. Soc. Jpn. Ser. II* 84, 247–258. <https://doi.org/10.2151/jmsj.84.247>.
- Knutson, T.R., McBride, J.L., Chan, J., Emanuel, K., Holland, G., Landsea, C., Held, I., Kossin, J.P., Srivastava, A.K., Sugi, M., 2010. Tropical cyclones and climate change. *Nat. Geosci.* 3, 157–163. <https://doi.org/10.1038/ngeo779>.
- Knutson, T., Camargo, S., Chan, J., Emanuel, K., Ho, C.-H., Kossin, J., Mohapatra, M., Satoh, M., Sugi, M., Walsh, K., Wu, L., 2019. Tropical cyclones and climate change assessment: Part I: Detection and attribution. *Bull. Am. Meteorol. Soc.* 100, 1987–2007. <https://doi.org/10.1175/BAMS-D-18-0189.1>.
- Knutson, T., Camargo, S., Chan, J., Emanuel, K., Ho, C.-H., Kossin, J., Mohapatra, M., Satoh, M., Sugi, M., Walsh, K., Wu, L., 2020. Tropical cyclones and climate change assessment: Part II: Projected response to anthropogenic warming. *Bull. Am. Meteorol. Soc.* 101, E303–E322. <https://doi.org/10.1175/BAMS-D-18-0194.1>.
- Kobayashi, S., Ota, Y., Harada, Y., Ebata, A., Moriya, M., Onoda, H., Onogi, K., Kamahori, H., Kobayashi, C., Endo, H., Miyaoka, K., Takahashi, K., 2015. The JRA-55 Reanalysis: General specifications and basic characteristics. *J. Meteorol. Soc. Jpn. Ser. II* 93 (1), 5–48. <https://doi.org/10.2151/jmsj.2015-001>.
- Kunkel, K., Karl, T., Brooks, H., Kossin, J., Lawrimore, J., Arndt, D., Bosart, L., Changnon, D., Cutter, S., Doesken, N., Emanuel, K., Groisman, P., Katz, R., Knutson, K., O'Brien, J., Paciorek, C., Peterson, T., Redmond, K., Robinson, D., Trapp, J., Vose, R., Weaver, S., Wehner, M., Wolter, K., Wuebbles, D., 2013. Monitoring and understanding trends in extreme storms: State of knowledge. *Bull. Am. Meteorol. Soc.* 94, 499–514. <https://doi.org/10.1175/BAMS-D-11-00262.1>.
- Kunreuther, H., Heal, G., Allen, M., Edenhofer, O., Field, C.B., Yohe, G., 2013. Risk management and climate change. *Nat. Clim. Change* 3, 447–450. <https://doi.org/10.1038/nclimate1740>.
- Kusunoki, S., Yoshimura, J., Yoshimura, H., Noda, A., Oouchi, K., Mizuta, R., 2006. Change of Baiu rain band in global warming projection by an atmospheric general circulation model with a 20-km grid size. *J. Meteorol. Soc. Jpn. Ser. II* 84, 581–611. <https://doi.org/10.2151/jmsj.84.581>.
- Kusunoki, S., Mizuta, R., Matsueda, M., 2011. Future changes in the East Asian rain band projected by global atmospheric models with 20-km and 60-km grid size. *Clim. Dynam.* 37, 2481–2493. <https://doi.org/10.1007/s00382-011-1000-x>.
- Lange, A., 2003. Climate change and the irreversibility effect - combining expected utility and MaxiMin. *Environ. Resour. Econ.* 25 (4), 417–434. <https://doi.org/10.1023/A:1025054716419>.
- Lempert, R.J., Groves, D.G., Popper, S.W., Bankes, S.C., 2006. A general, analytic method for generating robust strategies and narrative scenarios. *Manag. Sci.* 52 (4), 514–528. <https://doi.org/10.1287/mnsc.1050.0472>.
- Liang, Q., 2010. Flood simulation using a well-balanced shallow flow model. *J. Hydraul. Eng.* 136, 669–675. [https://doi.org/10.1061/\(ASCE\)HY.1943-7900.0000219](https://doi.org/10.1061/(ASCE)HY.1943-7900.0000219).
- Lin, N., Emanuel, K., Oppenheimer, M., Vanmarcke, E., 2012. Physically based assessment of hurricane surge threat under climate change. *Nat. Clim. Change* 2, 462–467. <https://doi.org/10.1038/nclimate1389>.
- Little, C.M., Horton, R.M., Kopp, R.E., Oppenheimer, M., Vecchi, G.A., Villarini, G., 2015. Joint projections of US East Coast sea level and storm surge. *Nat. Clim. Change* 5, 1114–1120. <https://doi.org/10.1038/nclimate2801>.
- Lowe, J.A., Gregory, J.M., 2005. The effects of climate change on storm surges around the United Kingdom. *Phil. Trans. R. Soc. A* 363, 1313–1328. <https://doi.org/10.1098/rsta.2005.1570>.
- Lowe, J.A., Bernie, D., Bett, P.E., Bricheno, L.M., Brown, S.C., Calvert, D., Clark, R., Eagle, K., Edwards, T.L., Fossier, G., Maisey, P., McInnes, R.N., Mcsweeney, C., Yamazaki, K., Belcher, S., 2019. UKCP 18 Science Overview Report: November 2018. Met Office Hadley Centre, Exeter, UK, p. 73 (Updated March 2019).
- Machina, M.J., Siniscalchi, M., 2014. Ambiguity and ambiguity aversion. In: Machina, M. J., Viscusi, W.K. (Eds.), *Handbook of the Economics of Risk and Uncertainty*, vol. 1. Elsevier, Amsterdam, pp. 729–807.
- Maher, N., Milinski, S., Suarez-Gutierrez, L., Botzet, M., Dobrynin, M., Kornbluh, L., Kröger, J., Takano, Y., Ghosh, R., Hedemann, C., Li, C., Li, H., Manzini, E., Notz, D., Putrasahan, D., Boysen, L., Claussen, M., Ilyina, T., Olonscheck, D., Raddatz, T., Stevens, B., Marotzke, J., 2019. The Max Planck Institute Grand Ensemble: Enabling the exploration of climate system variability. *J. Adv. Model. Earth Syst.* 11, 2050–2069. <https://doi.org/10.1029/2019MS001639>.
- McInerney, D., Lempert, R., Keller, K., 2012. What are robust strategies in the face of uncertain climate threshold responses? *Climatic Change* 112 (3–4), 547–568. <https://doi.org/10.1007/s10584-011-0377-1>.
- Meinke, I., Geyer, B., Feser, F., von Storch, H., 2006. The impact of spectral nudging on cloud simulation with a regional atmospheric model. *J. Atmos. Ocean. Technol.* 23, 815–824. <https://doi.org/10.1175/JTECH1879.1>.
- Merz, B., Thielen, A.H., 2009. Flood risk curves and uncertainty bounds. *Nat. Hazards* 51 (3), 437–458. <https://doi.org/10.1007/s11069-009-9452-6>.
- Miguez-Macho, G., Stenchikov, G.L., Robock, A., 2005. Regional climate simulations over North America: Interaction of local processes with improved large-scale flow. *J. Clim.* 18, 1227–1246. <https://doi.org/10.1175/JCLI3369.1>.
- Miyamoto, Y., Takemi, T., 2010. An effective radius of the sea surface enthalpy flux for the maintenance of a tropical cyclone. *Atmos. Sci. Lett.* 11, 278–282. <https://doi.org/10.1002/asl.292>.
- Mizuta, R., Arakawa, O., Ose, T., Kusunoki, S., Endo, H., Kitoh, A., 2014. Classification of CMIP5 future change climate responses by the tropical sea surface temperature changes. *SOLA* 10, 167–171. <https://doi.org/10.2151/sola.2014-035>.
- Mizuta, R., Murata, A., Ishii, M., Shiogama, H., Hibino, K., Mori, N., Arakawa, O., Imada, Y., Yoshida, K., Aoyagi, T., Kawase, H., Mori, M., Okada, Y., Shimura, T., Nagatomo, T., Ikeda, M., Endo, H., Nosaka, M., Arai, M., Takahashi, C., Tanaka, K., Takemi, T., Tachikawa, Y., Temur, K., Kamae, Y., Watanabe, M., Sasaki, H., Kitoh, A., Takayabu, I., Nakajima, E., Kimoto, M., 2017. Over 5000 years of ensemble future climate simulations by 60 km global and 20 km regional atmospheric models. *Bull. Am. Meteorol. Soc.* 98 (7), 1383–1398. <https://doi.org/10.1175/BAMS-D-16-0099.1>.
- Mizuta, R., Yoshimura, H., Murakami, H., Matsueda, M., Endo, H., Ose, T., Kamiguchi, K., Hosaka, M., Sugi, M., Yukimoto, S., Kusunoki, S., Kitoh, A., 2012. Climate simulations using MRI-AGCM3.2 with 20-km grid. *J. Meteorol. Soc. Jpn. Ser. II* 90A, 233–258. <https://doi.org/10.2151/jmsj.2012-A12>.
- Mori, N., Ariyoshi, N., Shimura, T., Miyashita, T., Ninomiya, J., 2021. Future projection of maximum potential storm surge height at three major bays in Japan using the maximum potential intensity of a tropical cyclone. *Climatic Change* 164 (25). <https://doi.org/10.1007/s10584-021-02980-x>.
- Mori, N., Kato, M., Kim, S., Mase, H., Shibutani, Y., Takemi, T., Tsuboki, K., Yasuda, T., 2014. Local amplification of storm surge by Super Typhoon Haiyan in Leyte Gulf. *Geophys. Res. Lett.* 41, 5106–5113. <https://doi.org/10.1002/2014GL060689>.
- Mori, N., Kjerland, M., Nakajo, S., Shibutani, Y., Shimura, T., 2016. Impact assessment of climate change on coastal hazards in Japan (review paper). *Hydrol. Res. Lett.* 10 (3), 101–105. <https://doi.org/10.3178/hrl.10.101>.
- Mori, N., Nakajo, S., Iwamura, S., Shibutani, Y., 2018. Projection of decrease in Japanese beaches due to climate change using a geographic database. *Coast Eng. J.* 60 (2), 239–246. <https://doi.org/10.1080/21664250.2018.1488513>.
- Mori, N., Shimura, T., Yoshida, K., Mizuta, R., Okada, Y., Fujita, M., Temur Khujanazarov, T., Nakajima, E., 2019. Future changes in extreme storm surges based on mega-ensemble projection using 60-km resolution atmospheric global circulation model. *Coast Eng. J.* 61 (3), 295–307. <https://doi.org/10.1080/21664250.2019.1586290>.
- Mori, N., Takemi, T., 2016. Impact assessment of coastal hazards due to future changes of tropical cyclones in the North Pacific Ocean. *Weather Clim. Extr.* 11, 53–69. <https://doi.org/10.1016/j.wace.2015.09.002>.
- Mori, N., Yasuda, T., Mase, H., Tom, T., Oku, Y., 2010. Projection of extreme wave climate change under the global warming. *Hydrol. Res. Lett.* 4, 15–19. <https://doi.org/10.3178/hrl.4.15>.
- Morim, J., Hemer, M., Xiaolan, L.W., Cartwright, N., Trenham, C., Semedo, A., Young, I., Bricheno, L., Camus, P., Casas-Prat, M., Erikson, L., Mentaschi, L., Mori, N., Shimura, T., Timmerman, B., Aarnes, O., Ø, Breivik, Behrens, A., Dobrynin, M., Mendez, M., Staneva, J., Wehner, M., Wolf, J., Kamranzad, B., Webb, A., Stopa, J., Andutta, F., 2019. Robustness and uncertainties in global multivariate wind-wave climate projections. *Nat. Clim. Change* 9, 711–718. <https://doi.org/10.1038/s41558-019-0542-5>.
- Morimoto, J., Nakagawa, K., Takano, K.T., Aiba, M., Oguro, M., Furukawa, Y., Mishima, Y., Ogawa, K., Ito, R., Takemi, T., Nakamura, F., Peterson, C.J., 2019. Comparison of vulnerability to catastrophic wind of Abies plantation forests and natural mixed forests in northern Japan. *Forestry: Int. J. For. Res.* 92, 436–443. <https://doi.org/10.1093/forestry/cpy045>.
- Muis, S., Verlaan, M., Winsemius, H.C., Aerts, J.C.J.H., Ward, P.J., 2016. A global reanalysis of storm surges and extreme sea levels. *Nat. Commun.* 7, 11969. <https://doi.org/10.1038/ncomms11969>.
- Murakami, H., Sugi, M., 2010. Effect of model resolution on tropical cyclone climate projections. *SOLA* 6, 73–76. <https://doi.org/10.2151/sola.2010-019>.
- Murphy, J.M., Sexton, D.M., Barnett, D.N., Jones, G.S., Webb, M.J., Collins, M., Stainforth, D.A., 2004. Quantification of modelling uncertainties in a large ensemble of climate change simulations. *Nature* 430, 768–772. <https://doi.org/10.1038/nature02771>.
- Nakajo, S., Mori, N., Yasuda, T., Mase, H., 2014. Global stochastic tropical cyclone model based on principal component analysis and cluster analysis. *J. Appl. Meteorol. Climatol. Am. Meteorol. Soc.* 53, 1547–1577. <https://doi.org/10.1175/JAMC-D-13-08.1>.
- Nakajima, E., Hashimoto, G., Morimoto, K., Osakada, Y., 2018a. An influence of atmospheric stabilization and vapor invasion on occurrence frequency of guerrilla-heavy rainfall. *J. Jpn. Soc. Civ. Eng. Ser. B1 Hydraul. Eng.* 74 (5), 125–130 (in Japanese). <https://doi.org/10.2208/jscejhe.74.5.125>.
- Nakajima, E., Kusano, H., Touge, Y., Kim, S., 2016. Future change in appearance frequency of atmospheric characteristics causing localized heavy rainfall during Baiu season using AGCM ensembles. *DPRI Annu. B*, 59B, pp. 230–248 (in Japanese, non-peer reviewed). <http://hdl.handle.net/2433/217295>.
- Nakajima, E., Miyake, T., Kim, K., Konoshima, L., 2012. Fundamental study on future change of localized heavy rainfall during Baiu due to climate change using a regional climate model. *J. Jpn. Soc. Civ. Eng. Ser. B1 Hydraul. Eng.* 68 (4), 1427–1432 (in Japanese). <https://doi.org/10.2208/jscejhe.68.4.1427>.
- Nakajima, E., Morimoto, K., Nosaka, M., 2018b. Analysis of the reproduction features of the guerrilla-heavy rainfall and estimation of future changes of the occurrence

- frequency in multi-resolution RCMs. DPRI Annu. B 61B, 479–499 (in Japanese, non-peer reviewed). <http://hdl.handle.net/2433/235865>.
- Nakakita, E., Morimoto, K., Touge, Y., 2017a. Estimation of future changes in the occurrence frequency of the guerrilla-heavy rainfall events using a 5-km-mesh regional climate model. *J. Jpn. Soc. Civ. Eng. Ser. B1 Hydraul. Eng.* 73 (4), 1133–1138 (in Japanese). <https://doi.org/10.2208/jscejhe.73.1.133>.
- Nakakita, E., Osakada, Y., 2018. Estimation of future changes in the heavy rainfall and atmospheric characteristics in Baiu season under climate change. *J. Jpn. Soc. Civ. Eng. Ser. B1 Hydraul. Eng.* 74 (4), 1139–1144 (in Japanese). <https://doi.org/10.2208/jscejhe.74.1.139>.
- Nakakita, E., Sato, H., Nishiwaki, R., Yamabe, H., Yamaguchi, K., 2017b. Early detection of baby-rain-cell aloft in a severe storm and risk projection for urban flash flood. *Adv. Meteorol.* 2017, 5962356. <https://doi.org/10.1155/2017/5962356>.
- Nayak, S., Dairaku, K., Takayabu, I., Suzuki-Parker, A., Ishizaki, N.N., 2018. Extreme precipitation linked to temperature over Japan: Current evaluation and projected changes with multi-model ensemble downscaling. *Clim. Dynam.* 51, 4385–4401. <https://doi.org/10.1007/s00382-017-3866-8>.
- Nayak, S., Takemi, T., 2019a. Dynamical downscaling of Typhoon Lionrock (2016) for assessing the resulting hazards under global warming. *J. Meteorol. Soc. Jpn. Ser. II* 97 (1), 69–88. <https://doi.org/10.2151/jmsj.2019-003>.
- Nayak, S., Takemi, T., 2019b. Quantitative estimations of hazards resulting from Typhoon Chanthu (2016) for assessing the impact in current and future climate. *Hydrol. Res. Lett.* 13, 20–27. <https://doi.org/10.3178/hrl.13.20>.
- Nayak, S., Takemi, T., 2020a. Robust responses of typhoon hazards in northern Japan to global warming climate: Cases of landfalling typhoons in 2016. *Meteorol. Appl.* 27, e1954. <https://doi.org/10.1002/met.1954>.
- Nayak, S., Takemi, T., 2020b. Clausius-Clapeyron scaling of extremely heavy rainfalls: Case studies of July 2017 and July 2018 heavy rainfall events over Japan. *J. Meteorol. Soc. Jpn. Ser. II* 98, 1147–1162. <https://doi.org/10.2151/jmsj.2020-058>.
- Nicholls, R.J., Hoozemans, F.M.J., Marchand, M., 1999. Increasing flood risk and wetland losses due to global sea-level rise: Regional and global analyses. *Global Environ. Change* 9, S69–S87. [https://doi.org/10.1016/S0959-3780\(99\)00019-9](https://doi.org/10.1016/S0959-3780(99)00019-9).
- Ninomiya, J., Mori, N., Takemi, T., Arakawa, O., 2017. SST ensemble experiment-based impact assessment of climate change on storm surge caused by pseudo-global warming: Case study of Typhoon Vera in 1959. *Coast Eng. J.* 59 (2), 1740002. <https://doi.org/10.1142/S0578563417400022>.
- Oddo, P.C., Lee, B.S., Garner, G.G., Srikrishnan, V., Reed, P.M., Forest, C.E., Keller, K., 2017. Deep uncertainties in sea-level rise and storm surge projections: Implications for Coastal Flood Risk Management. *Risk Anal.* 40, 153–168. <https://doi.org/10.1111/risa.12888>.
- Ohba, M., Sugimoto, S., 2019. Differences in climate change impacts between weather patterns: Possible effects on spatial heterogeneous changes of future extreme rainfall. *Clim. Dynam.* 52, 4177–4191. <https://doi.org/10.1007/s00382-018-4374-1>.
- Okada, Y., Takemi, T., Ishikawa, H., Kusunoki, S., Mizuta, R., 2017. Future changes in atmospheric conditions for the seasonal evolution of the Baiu as revealed from projected AGCM experiments. *J. Meteorol. Soc. Jpn. Ser. II* 95 (4), 239–260. <https://doi.org/10.2151/jmsj.2017-013>.
- Oku, Y., Takemi, T., Ishikawa, H., Kanada, S., Nakano, M., 2010. Representation of extreme weather during a typhoon landfall in regional meteorological simulations: A model intercomparison study for Typhoon Songda (2004). *Hydrol. Res. Lett.* 4, 1–5. <https://doi.org/10.3178/hrl.4.1>.
- Oku, Y., Yoshino, J., Takemi, T., Ishikawa, H., 2014. Assessment of heavy rainfall-induced disaster potential based on an ensemble simulation of Typhoon Talas (2011) with controlled track and intensity. *Nat. Hazards Earth Syst. Sci.* 14, 2699–2709. <https://doi.org/10.5194/nhess-14-2699-2014>.
- Osakada, Y., Nakakita, E., 2018a. Future change of occurrence frequency of Baiu heavy rainfall and its linked atmospheric patterns by multiscale analysis. *SOLA* 14, 79–85. <https://doi.org/10.2151/sola.2018-014>.
- Osakada, Y., Nakakita, E., 2018b. Future changes of “Baiu heavy rainfall duration and accumulated precipitation” using the regional climate model verified with past real heavy rainfall events. *J. Jpn. Soc. Civ. Eng. Ser. B1 Hydraul. Eng.* 74 (5), 119–124 (in Japanese). <https://doi.org/10.2208/jscejhe.74.5.119>.
- Osakada, Y., Nakakita, E., 2020. Multi-scale analysis on pseudo global warming experiment for back-building rainfall based on different resolutions. *J. Jpn. Soc. Civ. Eng. Ser. B1 Hydraul. Eng.* 76 (2), 1–6 (in Japanese).
- Ose, T., Takaya, Y., Maeda, S., Nakaegawa, T., 2020. Resolution of summertime East Asian pressure pattern and southerly monsoon wind in CMIP5 multi-model future projections. *J. Meteorol. Soc. Jpn. Ser. II* 98 (5), 927–944. <https://doi.org/10.2151/jmsj.2020-047>.
- Otte, T.L., 2008. The impact of nudging in the meteorological model for retrospective air quality simulations. Part I: Evaluation against national observation networks. *J. Appl. Meteorol. Climatol.* 47 (7), 1853–1867. <https://doi.org/10.1175/2007JAMC1790.1>.
- Peterson, T., Karl, T., Kossin, J., Kunkel, K., Lawrimore, J., McMahon, J., Vose, R., Yin, X., 2014. Changes in weather and climate extremes: State of knowledge relevant to air and water quality in the United States. *J. Air Waste Manag. Assoc.* 64 (2), 184–197. <https://doi.org/10.1080/10962247.2013.851044>.
- Pfahl, S., O’Gorman, P., Fischer, E., 2017. Understanding the regional pattern of projected future changes in extreme precipitation. *Nat. Clim. Change* 7, 423–427. <https://doi.org/10.1038/nclimate3287>.
- Resio, D.T., Irish, J.L., Westerink, J.J., Powell, N.J., 2013. The effect of uncertainty on estimates of hurricane surge hazards. *Nat. Hazards* 66, 1443–1459. <https://doi.org/10.1007/s11069-012-0315-1>.
- Roberts, M.J., Camp, J., Seddon, J., Vidale, P.L., Hodges, K., Vanniere, B., Mecking, J., Haarsma, R., Bellucci, A., Scoccimarro, E., Caron, L.P., Chauvin, F., Terray, L., Valcke, S., Moine, M.P., Putrasahan, D., Roberts, C., Senan, R., Zarzycki, C., Ullrich, P., 2020a. Impact of model resolution on tropical cyclone simulation using the HighResMIP-PRIMAVERA Multimodel Ensemble. *J. Clim.* 33 (7), 2557–2583. <https://doi.org/10.1175/JCLI-D-19-0639.1>.
- Roberts, M.J., Camp, J., Seddon, J., Vidale, P.L., Hodges, K., Vanniere, B., Mecking, J., Haarsma, R., Bellucci, A., Scoccimarro, E., Caron, L.P., Chauvin, F., Terray, L., Valcke, S., Moine, M.P., Putrasahan, D., Roberts, C., Senan, R., Zarzycki, C., Ullrich, P., Yamada, Y., Mizuta, R., Kodama, C., Fu, D., Zhang, Q., Danabasoglu, G., Rosenbloom, N., Wang, H., Wu, L., 2020b. Projected future changes in tropical cyclones using the CMIP6 HighResMIP Multimodel Ensemble. *Geophys. Res. Lett.* 47, e2020GL088662. <https://doi.org/10.1029/2020GL088662>.
- Rohmer, J., Cozannet, G.L., Manceau, J.C., 2019. Addressing ambiguity in probabilistic assessments of future coastal flooding using possibility distributions. *Climatic Change* 155, 95–109. <https://doi.org/10.1007/s10584-019-02443-4>.
- Rotunno, R., Emanuel, K.A., 1987. An air-sea interaction theory for tropical cyclones. Part II: Evolutionary study using a nonhydrostatic axisymmetric numerical model. *J. Atmos. Sci.* 44, 542–561. [https://doi.org/10.1175/1520-0469\(1987\)044<0542:AAITFT>2.0.CO;2](https://doi.org/10.1175/1520-0469(1987)044<0542:AAITFT>2.0.CO;2).
- Ryan, M.J., 2009. Generalizations of SEU: A geometric tour of some non-standard models. *Oxf. Econ. Pap.* 61 (2), 327–354. <https://doi.org/10.1093/oxep/gpn027>.
- Sasaki, H., Kurihara, K., Takayabu, I., Uchiyama, T., 2008. Preliminary experiments of reproducing the present climate using the Non-hydrostatic Regional Climate Model. *SOLA* 4, 25–28. <https://doi.org/10.2151/sola.2008-007>.
- Sato, T., Kimura, F., Kitoh, A., 2007. Projection of global warming onto regional precipitation over Mongolia using a regional climate model. *J. Hydrol.* 333, 144–154. <https://doi.org/10.1016/j.jhydrol.2006.07.023>.
- Schär, C., Frei, C., Lüthi, D., Davies, H.C., 1996. Surrogate climate-change scenarios for regional climate models. *Geophys. Res. Lett.* 23, 669–672. <https://doi.org/10.1029/96GL00265>.
- Schmeidler, D., 1989. Subjective probability and expected utility without additivity. *Econometrica* 57 (3), 571–587. <https://doi.org/10.2307/1911053>.
- Shen, W., Tuleya, R.E., Ginis, I., 2000. A sensitivity study of the thermodynamic environment on GFDL model hurricane intensity: Implications for global warming. *J. Clim.* 13, 109–121. [https://doi.org/10.1175/1520-0442\(2000\)013<0109:ASSOTT>2.0.CO;2](https://doi.org/10.1175/1520-0442(2000)013<0109:ASSOTT>2.0.CO;2).
- Shimizu, K., Yamada, T., Yamada, T., 2019. Projection for future change of confidence interval based on Bayesian statistics using a large ensemble dataset. *J. Jpn. Soc. Civ. Eng. Ser. B1 Hydraul. Eng.* 75 (2), 11301–11306. <https://doi.org/10.2208/jscejhe.75.2.1301>.
- Shimura, T., Mori, N., Mase, H., 2015a. Future projection of ocean wave climate: Analysis of SST impacts on wave climate changes in the western North Pacific. *J. Clim. Am. Meteorol. Soc.* 28, 3171–3190. <https://doi.org/10.1175/JCLI-D-14-01017.1>.
- Shimura, T., Mori, N., Mase, H., 2015b. Future projections of extreme ocean wave climates and the relation to tropical cyclones: Ensemble experiments of MRI-AGCM3.2H. *J. Clim. Am. Meteorol. Soc.* 28, 9838–9856. <https://doi.org/10.1175/JCLI-D-14-00711.1>.
- Shimura, T., Mori, N., Hemer, M.A., 2016a. Variability and future decreases in winter wave heights in the Western North Pacific. *Geophys. Res. Lett.* 43 (6), 2716–2722. <https://doi.org/10.1002/2016GL067924>.
- Shimura, T., Mori, N., Hemer, M.A., 2016b. Projection of tropical cyclone-generated extreme wave climate based on CMIP5 multi-model ensemble in the western North Pacific. *Clim. Dynam.* 49 (4), 1449–1462. <https://doi.org/10.1007/s00382-016-3390-2>.
- Skamarock, W.C., Klemp, J.B., Dudhia, J., Gill, D.O., Barker, D.M., Duda, M.G., Huang, X.Y., Wang, W., Powers, J.G., 2008. A Description of the Advanced Research WRF Version 3 (No. NCAR/TN-475+STR). University Corporation for Atmospheric Research. <https://doi.org/10.5065/D68S4MVH>.
- Srifer, R.L., Lempert, R.J., Wikman-Svahn, P., Keller, K., 2018. Characterizing uncertain sea-level rise projections to support investment decisions. *PLoS One* 13 (2), e0190641. <https://doi.org/10.1371/journal.pone.0190641>.
- Stauffer, D.R., Seaman, N.L., 1990. Use of four-dimensional data assimilation in a limited area mesoscale model. Part I: Experiments with synoptic-scale data. *Mon. Weather Rev.* 118, 1250–1277. [https://doi.org/10.1175/1520-0493\(1990\)118<1250:UOFDDA>2.0.CO;2](https://doi.org/10.1175/1520-0493(1990)118<1250:UOFDDA>2.0.CO;2).
- Stauffer, D.R., Seaman, N.L., 1994. Multiscale four-dimensional data assimilation. *J. Appl. Meteorol.* 33, 416–434. [https://doi.org/10.1175/1520-0450\(1994\)033<0416:MFDFA>2.0.CO;2](https://doi.org/10.1175/1520-0450(1994)033<0416:MFDFA>2.0.CO;2).
- Tachikawa, Y., Miyawaki, K., Tanaka, T., Yorozu, K., Kato, M., Ichikawa, Y., Kim, S., 2017. Future change analysis of extreme floods using large ensemble climate simulation data. *J. Jpn. Soc. Civ. Eng. Ser. B1 Hydraul. Eng.* 73 (3), 77–90 (in Japanese). <https://doi.org/10.2208/jscejhe.73.77>.
- Takano, K.T., Nakagawa, K., Aiba, M., Oguro, M., Morimoto, J., Furukawa, Y., Mishima, Y., Ogawa, K., Ito, R., Takemi, T., 2016. Projection of impacts of climate change on windthrows and evaluation of potential silvicultural adaptation measures: A case study from empirical modelling of windthrows in Hokkaido, Japan, by Typhoon Songda (2004). *Hydrol. Res. Lett.* 10, 138–144. <https://doi.org/10.3178/hrl.10.132>.
- Takayabu, I., Hibino, K., Sasaki, H., Shioyama, H., Mori, N., Shibutani, Y., Takemi, T., 2015. Climate change effects on the worst-case storm surge: A case study of Typhoon Haiyan. *Environ. Res. Lett.* 10, 064011. <https://doi.org/10.1088/1748-9326/10/6/064011>.
- Takemi, T., 2018a. The evolution and intensification of Cyclone Pam (2015) and resulting strong winds over the southern Pacific islands. *J. Wind Eng. Ind. Aerod.* 182, 27–36. <https://doi.org/10.1016/j.jweia.2018.09.007>.

- Takemi, T., 2018b. Importance of terrain representation in simulating a stationary convective system for the July 2017 Northern Kyushu Heavy Rainfall case. *SOLA* 14, 153–158. <https://doi.org/10.2151/sola.2018-027>.
- Takemi, T., 2019. Impacts of global warming on extreme rainfall of a slow-moving typhoon: A case study for Typhoon Talas (2011). *SOLA* 15, 125–131. <https://doi.org/10.2151/sola.2019-023>.
- Takemi, T., Ito, R., Arakawa, O., 2016a. Robustness and uncertainty of projected changes in the impacts of Typhoon Vera (1959) under global warming. *Hydrol. Res. Lett.* 10, 88–94. <https://doi.org/10.3178/hrl.10.88>.
- Takemi, T., Ito, R., Arakawa, O., 2016b. Effects of global warming on the impacts of Typhoon Mireille (1991) in the Kyushu and Tohoku regions. *Hydrol. Res. Lett.* 10, 81–87. <https://doi.org/10.3178/hrl.10.81>.
- Takemi, T., Okada, Y., Ito, R., Ishikawa, H., Nakakita, E., 2016c. Assessing the impacts of global warming on meteorological hazards and risks in Japan: Philosophy and achievements of the SOUSEI program. *Hydrol. Res. Lett.* 10, 119–125. <https://doi.org/10.3178/hrl.10.119>.
- Takemi, T., Yamasaki, S., 2020. Sensitivity of the intensity and structure of tropical cyclones to tropospheric stability conditions. *Atmosphere* 11 (411). <https://doi.org/10.3390/atmos11040411>.
- Takemi, T., Yoshida, T., Yamasaki, S., Hase, K., 2019. Quantitative estimation of strong winds in an urban district during Typhoon Jebi (2018) by merging mesoscale meteorological and large-eddy simulations. *SOLA* 15, 22–27. <https://doi.org/10.2151/sola.2019-005>.
- Tanaka, T., Kawai, Y., Tachikawa, Y., 2019. Evaluating reproducibility of annual maximum basin-averaged rainfall of d4PDF in all class-A rivers in Japan. *J. Jpn. Soc. Civ. Eng. Ser. B1 Hydraul. Eng.* 75 (2), 11135–11140 (in Japanese). https://doi.org/10.2208/jscejhe.75.2_11135.
- Tanaka, T., Tachikawa, Y., Ichikawa, Y., Yorozu, K., 2016. A flood risk curve development using conditional probability distribution of rainfall on duration. *J. Jpn. Soc. Civ. Eng. Ser. B1 Hydraul. Eng.* 72 (4), 11219–11224 (in Japanese). https://doi.org/10.2208/jscejhe.72.4_11219.
- Tanaka, T., Tachikawa, Y., Ichikawa, Y., Yorozu, K., 2018. Flood risk curve development with probabilistic rainfall modelling and large ensemble climate simulation data: A case study for the Yodo River basin. *Hydrol. Res. Lett.* 12 (4), 28–33. <https://doi.org/10.3178/hrl.12.28>.
- Tang, J., Wang, S., Niu, X., Hui, P., Zong, P., Wang, X., 2017. Impact of spectral nudging on regional climate simulation over CORDEX East Asia using WRF. *Clim. Dynam.* 48, 2339–2357. <https://doi.org/10.1007/s00382-016-3208-2>.
- Timmermans, B., Stone, D., Wehner, M., Krishnan, H., 2017. Impact of tropical cyclones on modeled extreme wind-wave climate. *Geophys. Res. Lett.* 44 (3), 1393–1401. <https://doi.org/10.1002/2016GL071681>.
- Tolman, H.L., 2009. User manual and system documentation of WAVEWATCH III version 3.14. Technical note. *MMAB Contrib.* 276, 220.
- Unuma, T., Takemi, T., 2016a. Characteristics and environmental conditions of quasi-stationary convective clusters during the warm season in Japan. *Q. J. R. Meteorol. Soc.* 142, 1232–1249. <https://doi.org/10.1002/qj.2726>.
- Unuma, T., Takemi, T., 2016b. A role of environmental shear on the organization mode of quasi-stationary convective clusters during the warm season in Japan. *SOLA* 12, 111–115. <https://doi.org/10.2151/sola.2016-025>.
- Unuma, T., Takemi, T., 2021. Rainfall characteristics and their environmental conditions during the heavy rainfall events over Japan in July 2017 of 2018. *J. Meteorol. Soc. Jpn. Ser. II* 99. <https://doi.org/10.2151/jmsj.2021-009>.
- USGCRP, 2018. Impacts, Risks, and Adaptation in the United States: Fourth National Climate Assessment, Volume II. In: Reidmiller, D.R., Avery, C.W., Easterling, D.R., Kunkel, K.E., Lewis, K.L.M., Maycock, T.K., Stewart, B.C. (Eds.). U.S. Global Change Research Program, Washington, DC, USA, p. 1515. <https://doi.org/10.7930/NCA4.2018>.
- von Storch, H., Langenberg, H., Feser, F., 2000. A spectral nudging technique for dynamical downscaling purposes. *Mon. Weather Rev.* 128, 3664–3673. [https://doi.org/10.1175/1520-0493\(2000\)128%3c3664:ASNTFD%3e2.0.CO;2](https://doi.org/10.1175/1520-0493(2000)128%3c3664:ASNTFD%3e2.0.CO;2).
- Waldron, K.M., Paegle, J., Horel, J.D., 1996. Sensitivity of a spectrally filtered and nudged limited-area model to outer model options. *Mon. Weather Rev.* 124, 529–547. [https://doi.org/10.1175/1520-0493\(1996\)124<0529:SOASFA>2.0.CO;2](https://doi.org/10.1175/1520-0493(1996)124<0529:SOASFA>2.0.CO;2).
- Weisse, R., von Storch, H., Feser, F., 2005. Northeast Atlantic and North Sea storminess as simulated by a regional climate model during 1958–2001 and comparison with observations. *J. Clim.* 18, 465–479. <https://doi.org/10.1175/JCLI-3281.1>.
- Withey, P., Sullivan, D., Lantz, V., 2019. Willingness to pay for protection from storm surge damages under climate change in Halifax Regional Municipality. *J. Environ. Manag.* 241, 44–52. <https://doi.org/10.1016/j.jenvman.2019.04.007>.
- Wong, T.E., Keller, K., 2017. Deep uncertainty surrounding coastal flood risk projections: A case study for New Orleans. *Earth's Future* 5 (10), 1015–1026. <https://doi.org/10.1002/2017EF000607>.
- Yamaguchi, M., Maeda, S., 2020a. Increase in the number of tropical cyclones approaching Tokyo since 1980. *J. Meteorol. Soc. Jpn. Ser. II* 98, 775–786. <https://doi.org/10.2151/jmsj.2020-039>.
- Yamaguchi, M., Maeda, S., 2020b. Slowdown of typhoon translation speeds in mid-latitudes in September influenced by the Pacific Decadal Oscillation and global warming. *J. Meteorol. Soc. Jpn. Ser. II* 98 (6), 1321–1334. <https://doi.org/10.2151/jmsj.2020-068>.
- Yang, J., Kim, S.Y., Mori, N., Mase, H., 2017. Bias correction of simulated storm surge height considering coastline complexity. *Hydrol. Res. Lett.* 11 (2), 121–127. <https://doi.org/10.3178/hrl.11.121>.
- Yang, J.A., Kim, S.Y., Mori, N., Mase, H., 2018. Assessment of long-term impact of storm surges around the Korean Peninsula based on a large ensemble of climate projections. *Coast Eng.* 142, 1–8. <https://doi.org/10.1016/j.coastaleng.2018.09.008>.
- Yasuda, T., Nakajo, S., Kim, S., Mase, H., Mori, N., Horsburgh, K., 2014. Evaluation of future storm surge risk in East Asia based on state-of-the-art climate change projection. *Coast Eng.* 83, 65–71. <https://doi.org/10.1016/j.coastaleng.2013.10.003>.
- Yasunaga, K., Sasaki, H., Wakazuki, Y., Kato, T., Muroi, C., Hashimoto, A., Kanada, S., Kurihara, K., Yoshizaki, M., Sato, Y., 2005. Performance of long-term integrations of the Japan Meteorological Agency nonhydrostatic model using the spectral boundary coupling method. *Weather Forecast.* 20, 1061–1072. <https://doi.org/10.1175/WAF894.1>.
- Yasunaga, K., Muroi, C., Kato, T., Yoshizaki, M., Kurihara, K., Kusunoki, S., Wakazuki, Y., Hashimoto, A., Kanada, S., Oouchi, K., Yoshimura, H., Mizuta, R., Noda, A., 2006. Changes in the Baiu frontal activity in the future climate simulated by super-high-resolution global and cloud-resolving regional climate models. *J. Meteorol. Soc. Jpn. Ser. II* 84 (1), 199–220. <https://doi.org/10.2151/jmsj.84.199>.
- Yatagai, A., Kamiguchi, K., Arakawa, O., Hamada, A., Yasutomi, N., Kitoh, A., 2012. APHRODITE: Constructing a long-term daily gridded precipitation dataset for Asia based on a dense network of rain gauges. *Bull. Am. Meteorol. Soc.* 93 (9), 1401–1415. <https://doi.org/10.1175/Bams-D-11-00122.1>.
- Yoshida, K., Sugi, M., Mizuta, R., Murakami, H., Ishii, M., 2017. Future changes in tropical cyclone activity in high-resolution large-ensemble simulations. *Geophys. Res. Lett.* 44 (19), 9910–9917. <https://doi.org/10.1002/2017GL075058>.
- Yoshida, T., Takemi, T., 2018. Properties of mixing length and dispersive stress in airflows over urban-like roughness obstacles with variable height. *SOLA* 14, 174–178. <https://doi.org/10.2151/sola.2018-031>.
- Yoshida, T., Takemi, T., Horiguchi, M., 2018. Large-eddy-simulation study of the effects of building height variability on turbulent flows over an actual urban area. *Bound. Layer Meteorol.* 168, 127–153. <https://doi.org/10.1007/s10546-018-0344-8>.